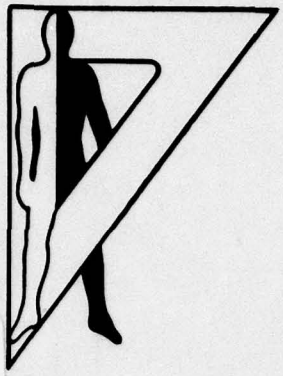

AD

LEVEL II

Technical Memorandum 8-79

EXPERIMENTAL IDLER DESIGN AND DEVELOPMENT OF HULL CONCEPTS FOR NOISE REDUCTION IN TRACKED VEHICLES

Thomas R. Norris
Peter E. Rentz
Anthony G. Galaitsis
Ronald B. Hare
Stephen A. Hammond
Georges R. Garinther

June 1979
AMCMS Code 612716.11.H700011

Approved for public release; distribution unlimited.

U. S. ARMY HUMAN ENGINEERING LABORATORY

Aberdeen Proving Ground, Maryland

Destroy this report when no longer needed.
Do not return it to the originator.

The findings in this report are not to be construed as an official Department of the Army position unless so designated by other authorized documents.

Use of trade names in this report does not constitute an official endorsement or approval of the use of such commercial products.

SECURITY CLASSIFICATION OF THIS PAGE *(When Data Entered)*

REPORT DOCUMENTATION PAGE

READ INSTRUCTIONS BEFORE COMPLETING FORM

1. REPORT NUMBER: Technical Memorandum 8-79

2. GOVT ACCESSION NO.:

3. RECIPIENT'S CATALOG NUMBER:

4. TITLE (and Subtitle): EXPERIMENTAL IDLER DESIGN AND DEVELOPMENT OF HULL CONCEPTS FOR NOISE REDUCTION IN TRACKED VEHICLES.

5. TYPE OF REPORT & PERIOD COVERED: Final rept.

6. PERFORMING ORG. REPORT NUMBER:

7. AUTHOR(s): Thomas R. Norris, Peter E. Rentz, Anthony G. Galaitsis, Ronald B. Hare, Stephen A. Hammond, Georges R. Garinther

8. CONTRACT OR GRANT NUMBER(s): DAAD05-77-C-0729

9. PERFORMING ORGANIZATION NAME AND ADDRESS: FMC Corporation, Ordnance Engineering Division, 1105 Coleman Avenue, San Jose, CA 95108

10. PROGRAM ELEMENT, PROJECT, TASK AREA & WORK UNIT NUMBERS: AMCMS Code 612716.11.H700011

11. CONTROLLING OFFICE NAME AND ADDRESS: U.S. Army Human Engineering Laboratory, Aberdeen Proving Ground, MD 21005

12. REPORT DATE: June 1979

13. NUMBER OF PAGES: 72

14. MONITORING AGENCY NAME & ADDRESS *(if different from Controlling Office)*: HEL TM-8-79

15. SECURITY CLASS. *(of this report)*: Unclassified

15a. DECLASSIFICATION/DOWNGRADING SCHEDULE:

16. DISTRIBUTION STATEMENT *(of this Report)*: Approved for public release; distribution unlimited.

74 p.

17. DISTRIBUTION STATEMENT *(of the abstract entered in Block 20, if different from Report)*:

18. SUPPLEMENTARY NOTES:

19. KEY WORDS *(Continue on reverse side if necessary and identify by block number)*:
Tracked Vehicles
Noise Reduction
Mechanical Impedance Measurement
Noise Sources
Track and Suspension
Statistical Energy Analysis

20. ABSTRACT *(Continue on reverse side if necessary and identify by block number)*:

Noise produced by track-laying vehicles is known to cause hearing loss, interfere with communications, and provide aural detectability to the enemy. The purpose of this program is to develop noise reduction concepts and to develop the technology necessary to produce a light, track-laying vehicle of the M113 family which has a sound level of 100 dB(A).

The first phase of this study rank ordered the major noise sources of the M113A1 Armored Personnel Carrier and developed a preliminary mathematical model of the track and suspension

(Continued)

DD FORM 1 JAN 73 1473 EDITION OF 1 NOV 65 IS OBSOLETE

402 012 LB

20. ABSTRACT (Continued)

system. Vibration-to-noise transfer functions were experimentally derived for inclusion in the model.

The present study was designed to capitalize upon those achievements by designing a high compliance idler, and by refining the computer model so that additional precision could be gained and a greater number of parameters varied. A power flow analysis of the hull was conducted along with structural modifications and damping treatment of a number of promising areas.

Computer runs were made to verify the model and to study the effect upon interior noise of several theoretical changes to the suspension system. Tests of the experimental compliant idler indicate that heat buildup and durability will not present problems. A cursory examination of its noise level indicated that this idler may provide significant noise reduction. Analysis of the acoustic and vibratory power flow was consistent, in that computed power radiated into the crew area agreed well with computed acoustic dissipation. However, due to the limited extent of the hull changes accomplished, the structural modifications provided no noise reduction and the damping treatment provided only slight noise reduction.

AMCMS Code 612716.11.H700011

Technical Memorandum 8-79

EXPERIMENTAL IDLER DESIGN AND DEVELOPMENT OF HULL CONCEPTS FOR NOISE REDUCTION IN TRACKED VEHICLES

Thomas R. Norris
Consultants in Engineering Acoustics

Peter E. Rentz
Anthony G. Galaitsis
Bolt, Beranek, and Newman, Inc.

Ronald B. Hare
Stephen A. Hammond
FMC Corporation

Georges R. Garinther

June 1979

APPROVED:
JOHN D. WEISZ
Director
U. S. Army Human Engineering Laboratory

U. S. ARMY HUMAN ENGINEERING LABORATORY
Aberdeen Proving Ground, Maryland 21005

CONTENTS

FIGURES (Continued)

TABLES

EXECUTIVE SUMMARY

The conclusions reached in this study are summarized below:

1. The statistical energy analysis of the acoustic and vibratory power flows were self-consistent. That is, the calculated acoustic power radiated into the crew area agrees well with the calculated acoustic dissipation.

2. A damping treatment applied to both sponsons provided appreciable sponson vibration reduction at 500 Hz and higher frequencies. This treatment also gave a modest vibration reduction of other hull plates, and noise reduction of approximately 0-2 dB(A).

3. Very careful control of testing parameters is necessary to accurately measure the incremental noise reductions that must be evaluated, such as would be necessary to confirm the above estimated noise reduction.

4. To achieve appreciable noise reduction by means of hull plate damping, a promising technique is constrained layer damping.

5. A damping treatment of the roadwheels was found to reduce roadwheel resonant amplitudes when vibrated by an electrodynamic shaker. Further experimentation is needed to determine if a corresponding crew area noise reduction could be obtained.

6. Local stiffening of the hull at the roadarm and idler mounting locations provided no significant changes to the mechanical impedances and, therefore, no noise reduction potential.

7. Vehicle interior sound absorptive treatments are not practical.

8. A very compliant low-noise idler wheel was designed, fabricated, and found to be rugged enough for extensive acoustical testing. Preliminary measurements suggest that the compliant wheel is about 10 dB(A) quieter than the standard idler wheel.

9. The best spring material for compliant idlers and sprockets appears to be either natural or synthetic base "natural" rubber. Steel springs would be difficult to engineer into the limited space available.

10. A number of highly resilient elastomers were also evaluated as spring materials, but were found to have inferior mechanical or damping properties.

11. In the compliant idler wheel, side-to-side as well as radial and tangential compliance must be considered.

12. The computerized simulation of track dynamics, while producing promising results, would require incremental refinement before it should be used in designing lower noise suspension components.

Based on these conclusions, a quieted demonstration vehicle might include compliant idler and sprocket wheels to reduce hull force inputs, a hull damping treatment to reduce hull vibration and a modified hull structure to reduce both hull vibration and noise radiated into the occupied areas.

EXPERIMENTAL IDLER DESIGN AND DEVELOPMENT OF HULL CONCEPTS FOR NOISE REDUCTION IN TRACKED VEHICLES

OBJECTIVE AND GOALS

The basic objective of this program was to develop concepts that will result in developing a lightweight tracked vehicle that will permit crew members to perform their duties without the additional use of hearing protectors. They are presently required to use hearing protectors in addition to the DH132 Combat Vehicle Crewman's Helmet. Reduction of the interior noise level would also improve communication between crew members.

Accordingly, the interior noise goal has been set at 100 dB(A), in conformance with the guidelines of MIL-STD-1474A, Category B. Achievement of this goal requires a 17 dB(A) noise reduction, primarily at low frequencies. In a weight-critical machine designed for survivability in an extreme environment, this represents a major technical challenge.

The U.S. Army Human Engineering Laboratory (HEL) has recognized that practical design modifications required to achieve significant interior noise reductions do not exist at present. It was also realized that the development of these noise controls must be based on experimental and analytical evaluations of both the noise sources and their transmission paths. Studies prior to the HEL sponsored work (e.g., References 1, 11, 23 and 25) had identified the major noise sources but had not quantified their contributions. A preceding study by FMC Corporation, sponsored by HEL, identified the separate contributions to interior noise generated by the idlers, the sprockets, and the roadwheels. This work also identified several promising concepts for tracked vehicle noise reduction.

The M113A1 vehicle was chosen as the demonstration vehicle for this study because it was used in a previous HEL-sponsored study, because of vehicle availability, and because of the relative availability and low cost of replacement parts. However, all noise reducing concepts developed in this study could be adapted to other tracked vehicles with suitable scaling changes.

Only suspension noise sources were considered in this study. Previous studies (3, 16) have shown that other noise sources are secondary; such as the engine, powertrain, and final drive gearing. Furthermore, these suspension noise sources are common to high-speed tracked vehicle noise problems and the technology needed to successfully reduce the noise from these sources does not exist at present. Developing practical noise controls for these suspension noise sources is the fundamental purpose of this program.

This present work is largely based on the results of a preceding HEL sponsored program which identified the noise sources, their levels, and promising techniques for noise controls (16). A computerized track dynamic analysis was also begun. The most important conclusions obtained from that research were:

1. At and below 20 mph, idler and sprocket noise must both be reduced to meet the noise reduction goals.

2. Above 20 mph, roadwheel noise must also be controlled in addition to idler and sprocket noise.

3. Making the idler and sprocket wheel rims more compliant is an effective and promising noise reduction technique.

4. Engine and power train noise is not significant compared to suspension induced noise.

5. The technology to reduce tracked vehicle noise does not exist and will require development.

The reported program extends the previous work. The purposes are to gain a better understanding of the track noise generation mechanisms, how the suspension vibration is conveyed throughout the hull and can be reduced by hull changes, and to demonstrate the feasibility of a compliant idler wheel. This research was divided into three somewhat independent tasks, each of which could help reduce noise. These tasks were to:

1. Analyze the vibratory power flow in the M113A1 hull, evaluate experimental damping treatments, and evaluate experimental hull modifications.

2. Design and fabricate an experimental low-noise compliant idler wheel.

3. Predict the effects of idler wheel modifications on track-induced interior noise by using a numerical computer simulation of track motion around the idler and sprocket wheels.

The first task developed a better understanding of how hull vibration contributed to interior noise. In addition, the hull damping and structural modifications performed for diagnostic purposes had potential applicability as noise control measures.

The second task demonstrated that a compliant-rimmed idler wheel is mechanically feasible and would result in significantly lower noise.

The third of the above tasks was to analytically evaluate the noise reductions of idler and sprocket wheel modifications by a computer analysis. While requiring further refinement, the analysis has produced basically correct results.

In this project the FMC Corporation, the producer of the M113A1 vehicle, was the prime contractor and provided design, test, and fabrication assistance and overall management of the program. The power vibratory flow analysis was conducted by Mr. Peter Rentz of Bolt Beranek & Newman, Inc., Canoga Park, and the computer analysis was conducted by Dr. Anthony Galaitsis of Bolt Beranek & Newman, Inc., Cambridge. The idler wheel design analysis and coordination regarding the computer analysis, were conducted by Mr. Thomas Norris of Consultants in Engineering Acoustics.

DISCUSSION OF TRACKED VEHICLE INTERIOR NOISE

General Discussion

Interior noise in tracked vehicles results from track interaction with the drive sprockets, idler wheels, and roadwheels. The engine and powertrain is a secondary noise source in most tracked vehicles. Some vehicles, such as the M60 tank and mechanized infantry combat vehicle (MICV), have track support rollers which may also produce significant interior noise. Figure 1 is a schematic representation of tracked vehicle noise sources and vibration paths.

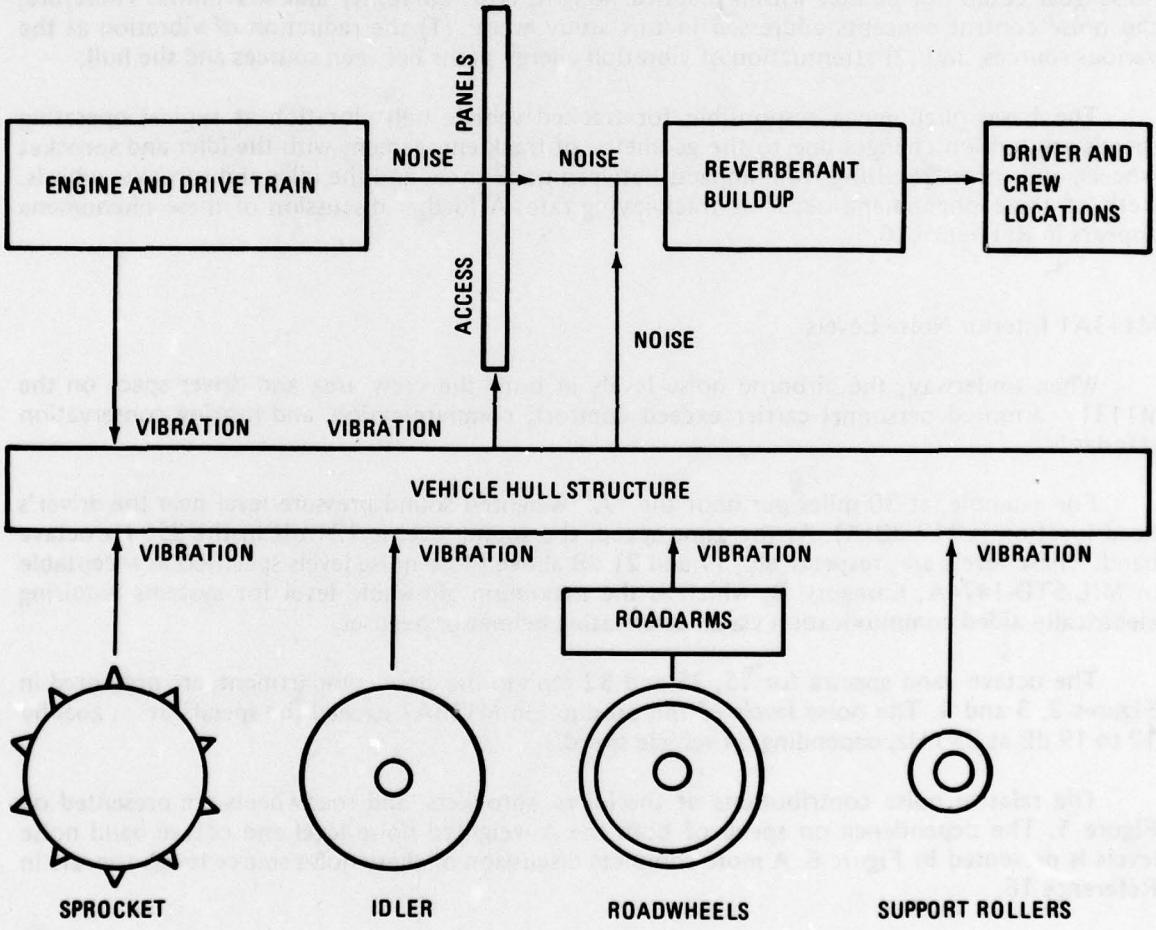

Figure 1. Schematic diagram of sources and paths responsible for interior noise in tracked vehicles.

Noise in moving tracked vehicles results from vibration of the hull which is excited by suspension and engine-powertrain components. The hull structure distributes vibration energy from each source to the remainder of the hull which, in turn, radiates noise. The interior noise levels at the driver and crew locations are established by the direct radiation of sound from the hull surfaces and by reverberant buildup.

Accordingly, noise control in lightweight tracked vehicles is more a matter of reducing hull vibration than installing barriers or absorbers. Consideration of "conventional" acoustic noise control barriers and absorbers showed that, because the entire hull radiates noise, the 100 dB(A) noise goal could not be met within practical weight, cost, durability and size limits. Therefore, the noise control concepts addressed in this study were: (1) the reduction of vibration at the various sources, and (2) attentuation of vibration energy paths between sources and the hull.

The basic phenomena responsible for tracked vehicle hull vibration at typical operating speeds are tension changes due to the geometry of track engagement with the idler and sprocket wheels, and forces resulting from impacts between track shoes and the idler and sprocket wheels. Both of these phenomena occur at track-laying rate. A further discussion of these phenomena appears in Reference 16.

M113A1 Interior Noise Levels

When underway, the airborne noise levels in both the crew area and driver space on the M1131 armored personnel carrier exceed comfort, communication, and hearing conservation standards.

For example, at 30 miles per hour the "A" weighted sound pressure level near the driver's head location is 117 dB(A). At the same speed, the sound level is 124 dB in the 250 Hz octave band. These levels are, respectively, 17 and 21 dB above those noise levels specified as acceptable in MIL-STD-1474A, Category B, which is the maximum allowable level for systems requiring electrically aided communication via an attenuating helmet or headset.

The octave band spectra for 15, 25 and 32 mph in the crew compartment, are presented in Figures 2, 3 and 4. The noise levels of the production M113A1 exceed the specification goal by 12 to 19 dB at 250 Hz, depending on vehicle speed.

The relative noise contributions of the idlers, sprockets, and roadwheels are presented on Figure 5. The dependence on speed of both the A-weighted noise level and octave band noise levels is presented in Figure 6. A more complete discussion of these noise source levels appears in Reference 16.

STATISTICAL POWER FLOW ANALYSIS AND HULL MODIFICATIONS

Background

This section documents application of the statistical energy power flow theory to the M113A1 hull and suspension. A theoretical discussion of statistical energy analysis is presented as the appendix.

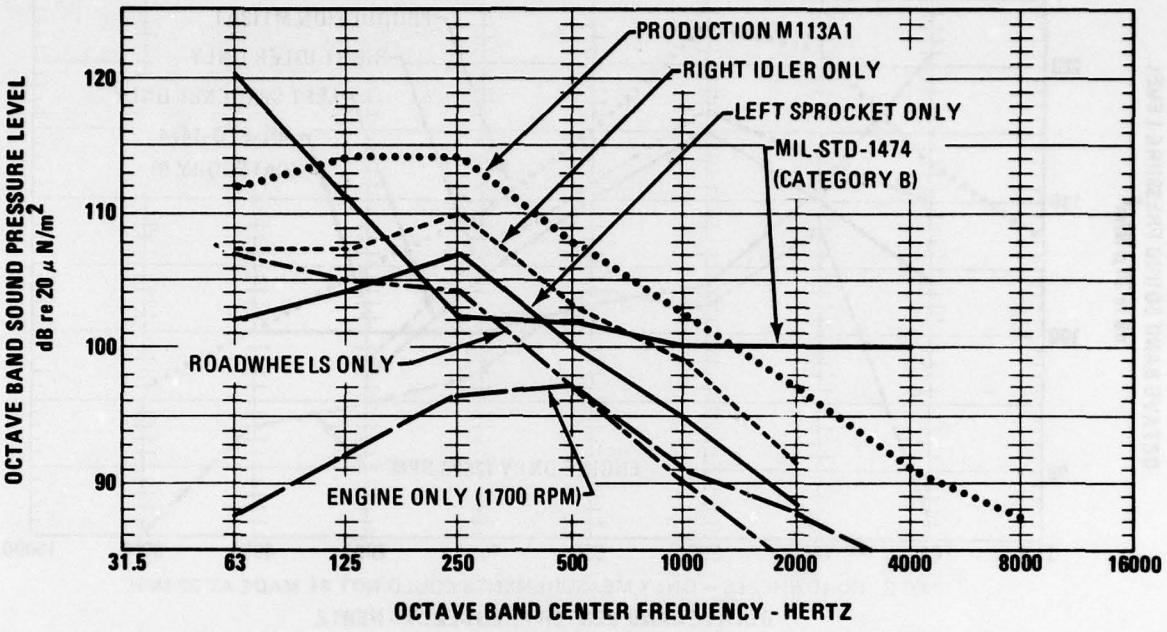

Figure 2. Noise source spectra at 15 MPH at center of crew compartment.

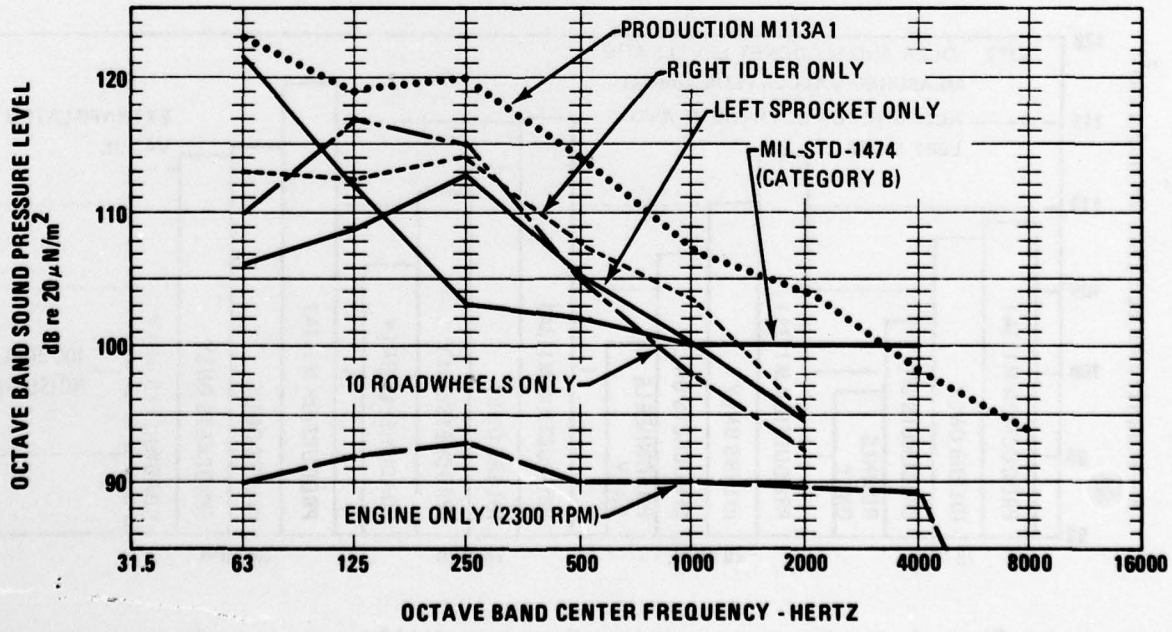

Figure 3. Noise source spectra at 25 MPH at center of crew compartment.

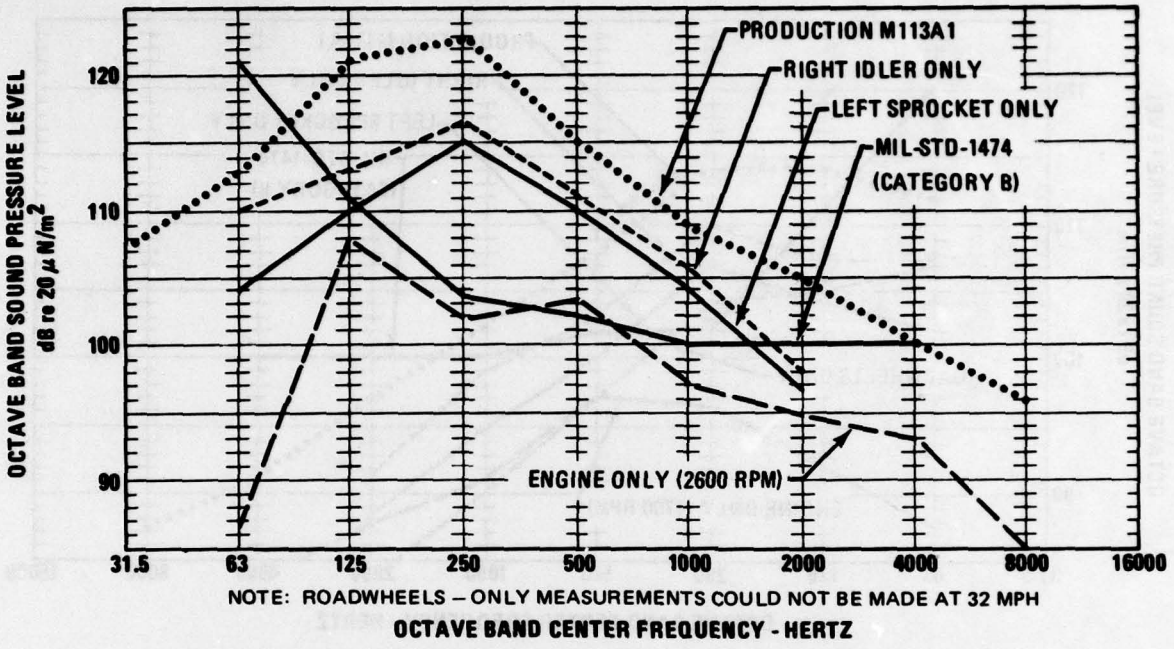

Figure 4. Noise source spectra at 32 MPH at center of crew compartment.

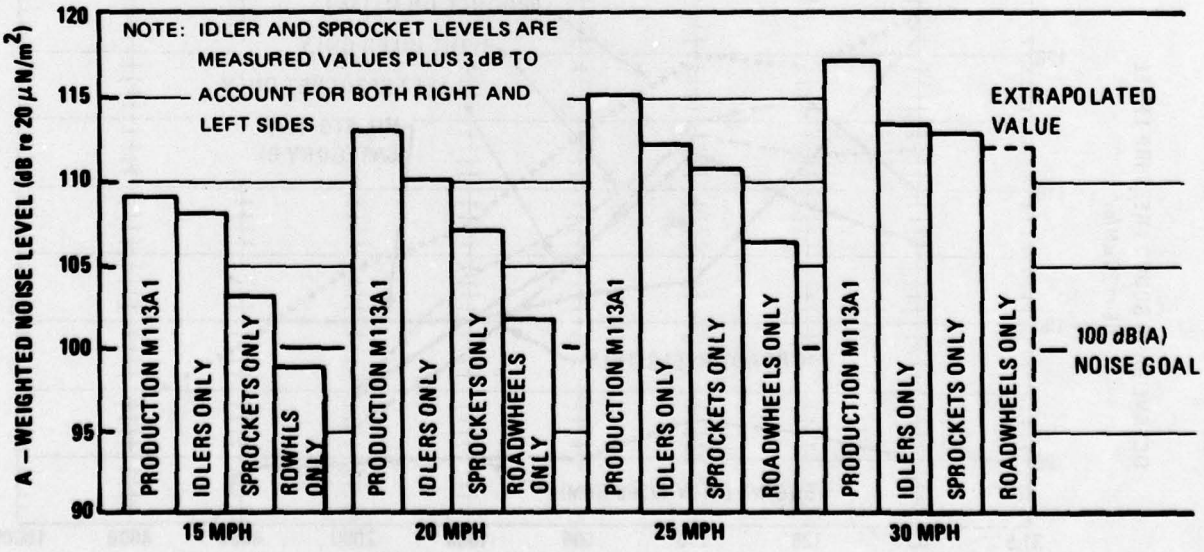

Figure 5. Track system source contributions to M113A crew area noise levels at various speeds.

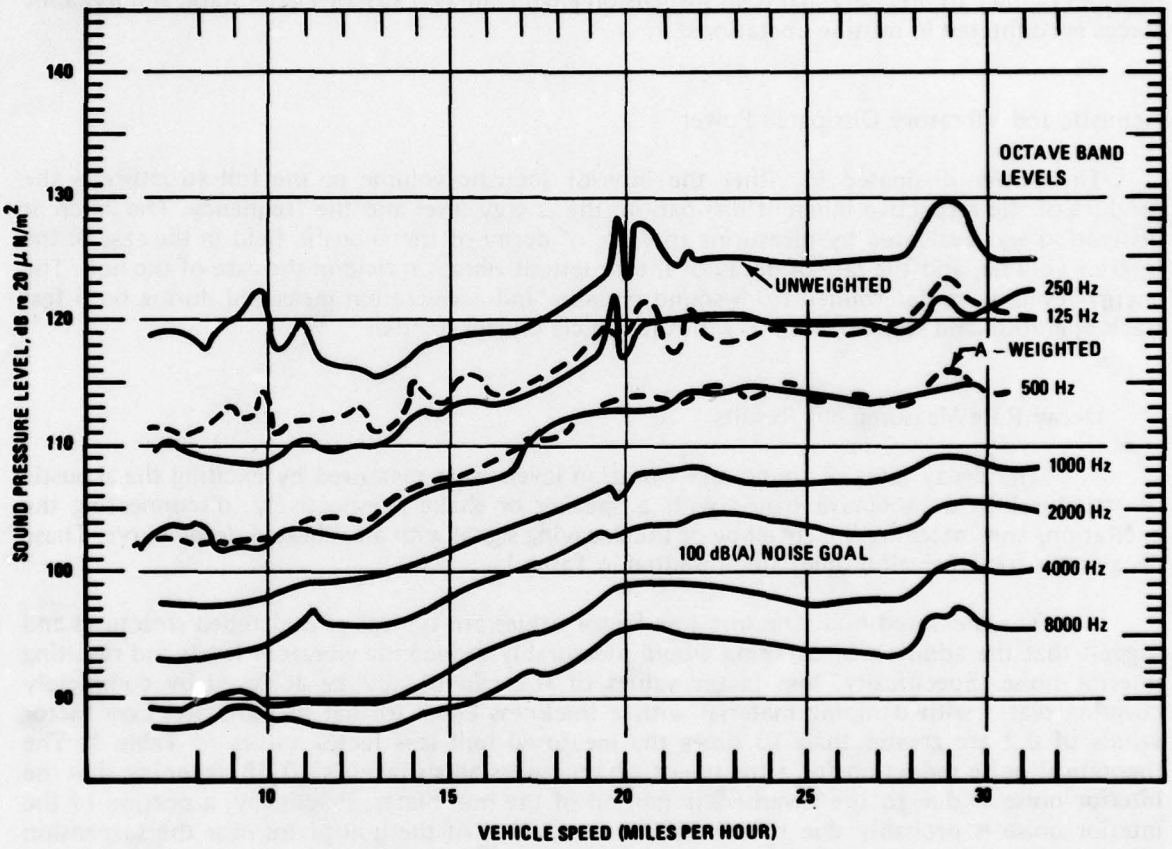

Figure 6. Speed dependence of production M113A1 noise at the crew position operating on paved track.

The cross section of the vehicle (Figure 7), gives an appreciation of the nature of the vibratory power input and distribution patterns. The roadwheel bearings and idler spindles are bolted directly to longitudinal box beams. The idler attachment is at the intersection of the back, bottom and lower side plates. The sprocket is supported by a final drive housing containing large reduction gears, which is bolted to the hull at the front of the vehicle. In all three cases, extremely good mechanical coupling exists between the suspension members and the hull. In addition, all hull plates are welded together, with flanking paths at the front and aft. This design has proved to be extremely successful for durability and maintainability. The hull structure provides rigidity to precisely maintain suspension alignment as it sustains large static and dynamic forces encountered in routine operations.

Acoustic and Vibratory Dissipated Power

The power dissipated in either the interior acoustic volume or the full structure is the product of the respective inherent dissipation, the energy level and the frequency. The inherent dissipation was evaluated by measuring the rate of decay of the acoustic field in the case of the interior volume, and the rate of decay of the structural vibration field in the case of the hull. The energy levels were determined from sound pressure and acceleration measured during both test track operation and static operation with the vehicle on jackstands.

Decay Rate Measurement Results

The decay rates of sound and vibration levels were measured by exciting the acoustic or structural field in octave bands with a speaker or shaker, respectively, disconnecting the excitation, and matching the envelope of the decaying signal with a calibrated decay curve. These decay rates (reverberation time) are presented in Table 1.

The measured hull structure loss factor values are typical of undamped structures and suggest that the addition of damping would measurably reduce the vibratory levels and resulting interior noise. Specifically, loss factor values of 0.2 can usually be achieved by completely covering plates with damping material with a thickness equal to that of the plate. Loss factor values of 0.2 are greater than 10 times the measured hull loss factor values of Table 1. The theoretical noise reduction for a treatment which covers all surfaces is 10 dB assuming that the interior noise is due to the reverberant motion of the hull plates. Practically, a portion of the interior noise is probably due to nonreverberant motion of the hull plates near the suspension attachments, and less than 10 dB reduction could be realized for such a treatment.

For the reverberant interior acoustic field, average surface absorption values were calculated from reverberation times measured with one and three people present in the crew space (Table 1). In addition, the ratio of absorption values expressed in dB is presented. Finally, the distance from an acoustic radiating point on a hull plate to where the direct and reverberant acoustic fields are theoretically equal in level was determined for each octave band and listed in Table 1. This distance is known as the "Hall Radius."

The average interior surface absorption coefficient values are low as would be expected in a hard-walled box. This suggests that significant reduction of interior noise could be achieved with the addition of sound absorbing material. This expectation is reduced somewhat because of the absorption afforded by the crew. For example, covering the top plate with 70 square feet of 90 percent absorptive foam would more than double the absorption measured with three people present. This would effect a three dB (or greater) reduction of the reverberant noise field.

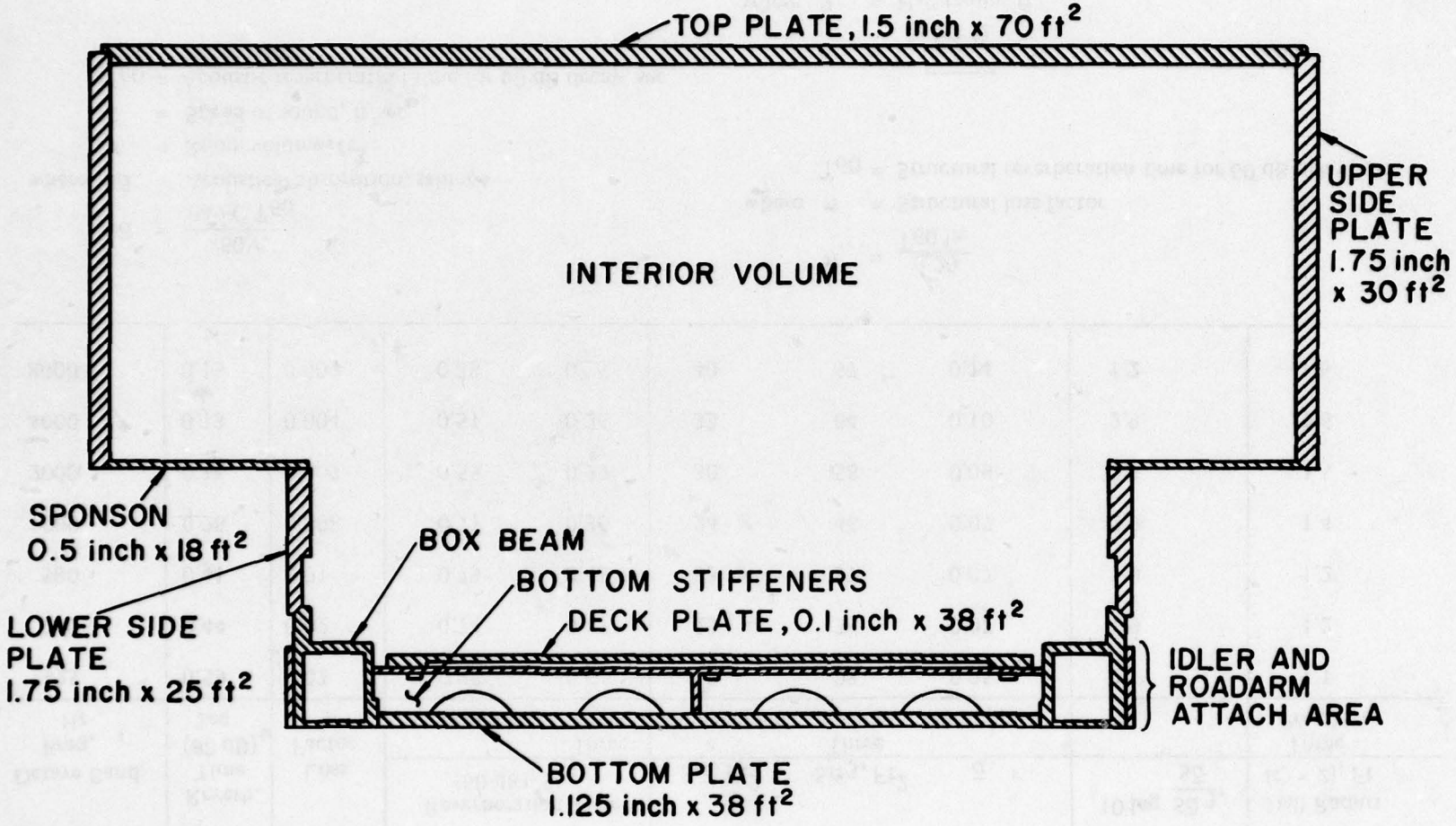

Figure 7. Cross section of the M113A hull showing major plates and suspension attachment area.

TABLE 1

Reverberation Times and Loss Factor Values of Interior Acoustic Volume and Hull Structure

Hull Structure			Hull Interior Volume Properties						
Octave Band Freq, Hz	Reverb. Time (60 dB), Sec	Loss Factor η	Reverberation Time (60 dB), Sec		$S\bar{\alpha}$, Ft^2	$S\bar{\alpha}_3$, Ft^2	$\bar{\alpha}$	$10 \log \frac{S\bar{\alpha}_3}{S\bar{\alpha}}$,	Hall Radius (Q = 2), Ft
			Unoccupied	Three People	Unoccupied	Three People	Unoccupied	dB	Three People
125	0.59	0.03	0.98	0.6	17	28	0.05	2.1	1.1
250	0.44	0.02	0.74	0.47	23	36	0.07	1.9	1.2
500	0.41	0.01	0.73	0.45	23	37	0.07	1.0	1.2
1000	0.28	0.008	0.71	0.36	24	46	0.07	2.9	1.4
2000	0.16	0.007	0.55	0.29	30	58	0.09	2.3	1.5
4000	0.13	0.004	0.51	0.26	33	64	0.10	2.9	1.6
8000	0.13	0.002	0.38	0.25	40	67	0.14	1.2	1.6

$$S\bar{\alpha} = \frac{60V}{.049\, C\, T_{60}}$$

where $S\bar{\alpha}$ = Acoustical absorption, sabines

V = Room volume, ft^3

C = Speed of sound, ft/sec

T_{60} = Acoustic reverberation time for 60 dB decay, sec

$$\eta = \frac{2.20}{T_{60} f_n}$$

where η = Structural loss factor

T_{60} = Structural reverberation time for 60 dB delay, sec

$$R = 4\sqrt{\frac{\pi}{S\bar{\alpha}\, Q}}$$

where R = Hall radius, ft

Q = Assumed directivity

However, since the interior noise also consists of a direct sound field which is not reduced by sound absorptive treatments, the actual noise reduction could be less.

Without exhaustive analysis, the noise reduction in the crew area is estimated to be one-half of the reverberant noise reduction calculated from absorption values (in dB). Any estimate of the effectiveness of additional absorption should similarly be tempered. In addition, achieving large absorption coefficients at frequencies as low as 250 Hz requires treatments roughly 3 inches thick, which would consume already limited interior space. In summary, the interior volume sound decay rate measurements show that the reverberant interior acoustic field is dominant, but that noise reduction by the addition of absorbing material has serious practical limitations, and therefore, is not recommended.

Track Operation: Results of Measurements and Dissipated Power Calculation

Interior acoustic and hull vibration acceleration signals were tape recorded with the vehicle underway and while mounted on jackstands. Approximately 40 measurement locations were required to define the motion of the 13 major radiating interior panels. Therefore, in order to keep the results tractable, the evaluation was limited to one speed, 20 mph. The tape recorded signals were then analyzed in octave bands. The noise levels were compared to those of Figure 6 and found consistent. For a point of physical reference panel acceleration levels averaged 5 dB re 1.0 g in the 250 Hz octave band and 10 dB re 1.0 g overall.

Acoustic dissipated power values were calculated from the octave band sound level measurements and the loss factor values of Table 1 and are presented in Figure 8 as the dash-dot curve.

Structural dissipated power levels for individual panels were similarly derived from averaged panel octave band acceleration measurements. The panel power levels were summed to arrive at the total hull vibratory power and are also presented in Figure 8. This figure also shows the total calculated power radiated from the hull panels into the interior acoustic volume. The calculation used the aforementioned averaged vibration levels and the radiation efficiencies of the individual panels (Tables 2, 3 and 4). The radiation efficiencies of the integral hull panels were determined analytically. The radiation efficiencies of various lightweight panels such as the deck were experimentally determined by attaching an electrodynamic shaker to each panel and vibrating the panel using octave bands of pink noise. The resulting panel acceleration levels and the sound levels in the crew space were then measured and the radiation efficiencies calculated using the previously measured sound power and sound pressure calibrations of the crew space.

Figure 8 shows that the acoustic power dissipated in the internal volume matches the power radiated from the panels. This is important because it gives confidence in the calculation of the relative contributions of the individual plates. Figure 8 also shows that the power dissipated in the hull is significantly greater than the acoustic radiated power, as would be expected. However, if the plate radiation is increased by 3 dB to account for radiation from both sides of the plates, it becomes apparent that acoustic radiation is contributing measurably to the hull dissipation.

For the purposes of noise control, the contributions of the individual panels are even more interesting than the total radiated power. The individual calculated hull panel contributions to the interior noise levels are shown in Figure 9. The top plate, upper side plates, and lower side plates were similar in level and only their average is shown. Many panels contribute to the

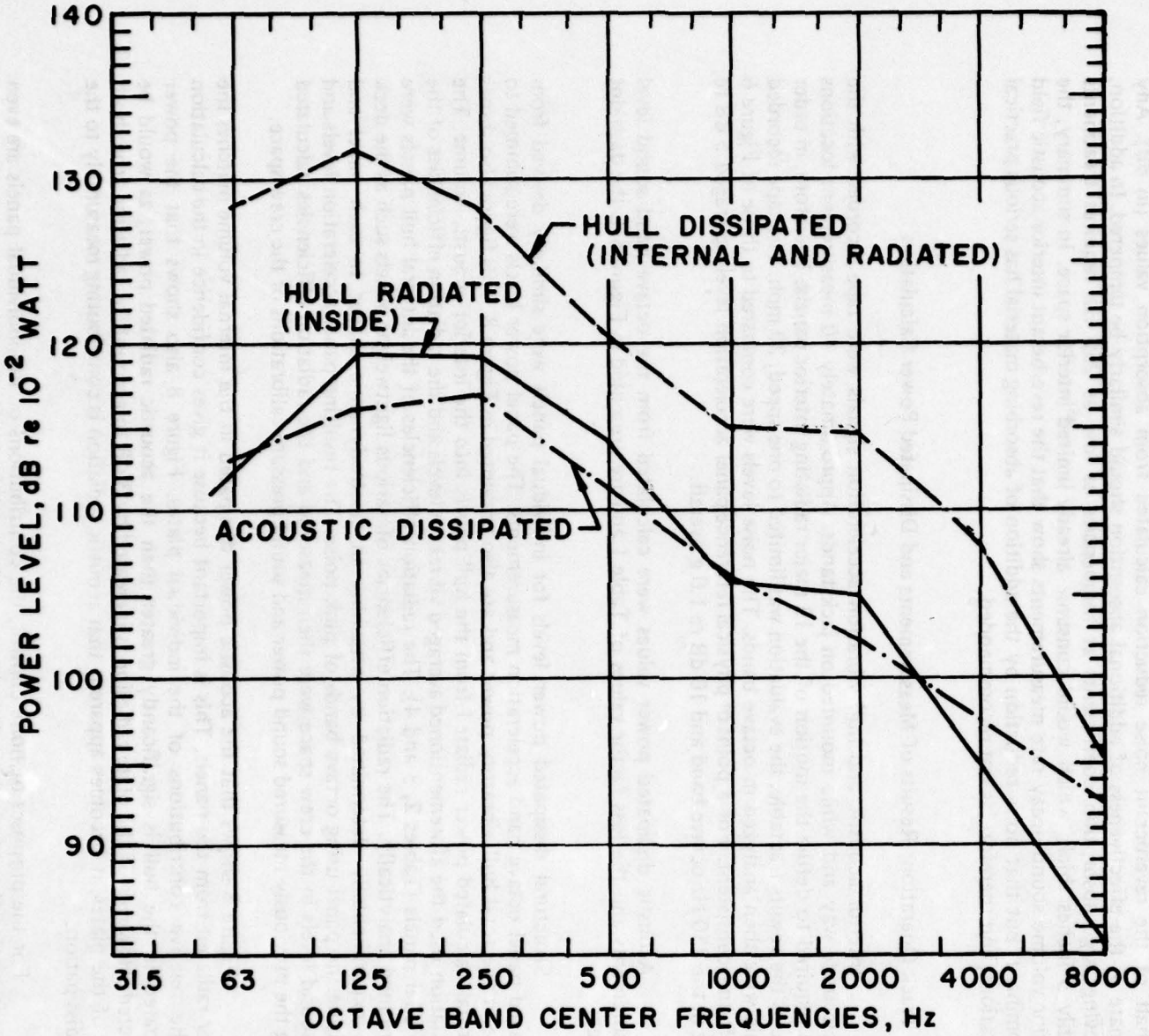

Figure 8. Comparison of hull dissipated, hull radiated, and acoustic dissipated power values, baseline vehicle at 20 MPH, vehicle self-powered while supported on jackstands.

TABLE 2

Space Averaged Vibration Acceleration Level, dB re 1.0g rms, for the Baseline Vehicle at 20 Miles Per Hour

Panel	Area Ft^2	Octave Band Center Frequency, Hz							
		63	125	250	500	1K	2K	4K	8K
Bottom	38.0	-2.5	5.0	4.5	4.5	2.5	4.0	-0.5	-4.5
Deck (1)	13.0	2.5	10.0	9.5	9.0	2.0	5.0	-3.5	-12.0
Lower Side	25.4	-6.0	1.0	1.0	3.5	4.5	10.0	4.0	0
Sponsons	28.4	-6.5	2.0	1.5	11.0	6.0	12.0	7.5	1.0
Upper Side	61.0	-8.5	2.0	3.0	3.0	-1.0	3.0	-2.0	-7.5
Top	70.0	-4.0	5.5	3.5	3.5	0	2.5	-2.5	-3.0
Bulkhead	14.5	-11.0	-1.5	6.5	7.0	2.0	8.0	6.5	4.0
Access Panels	14.5	-3.0	6.0	12.0	10.0	3.5	2.5	-5.5	-10.0
Fuel Tank Cover	11.0	3.0	14.0	13.0	10.5	5.0	1.0	-3.5	-3.5
Nose	11.0	-11.0	-5.5	9.5	4.0	-0.5	2.5	-2.5	-5.0
Aft	35.0	-13.0	1.5	5.0	1.5	0.5	-4.0	-3.5	-6.5
Ramp	13.3	-9.0	-8.0	-1.5	-2.0	-6.0	-4.0	-7.0	-5.5
Door	6.7	-9.5	-6.0	-6.0	-5.0	-11.0	-10.5	-16.0	-16.5

TABLE 3

Panel Radiation Efficiency[a]
(10 log σ, dB re 1.0)

Panel	Critical Frequency Hz	Octave Band Center Frequency, Hz							
		63	125	250	500	1K	2K	4K	8K
Bottom	439	-12	-11	-6	0	0	0	0	0
Deck (1)[b]	4960	-18	-11	-5.5	-2.5	-2.5	1.5	8.5	9
Lower Side	282	-5	-3	0	0	0	0	0	0
Sponsons	988	-13	-12	-11	-7	0	0	0	0
Upper Side	282	-8	-5	0	0	0	0	0	0
Top	329	-12	-9	-2	0	0	0	0	0
Bulkhead	1976	-16	-15	-14	-12.5	-8.5	0	0	0
Access Panels[b]	8200	-19	-17	-15	-9	-6	1	2	-3
Fuel Tank Cover[b]	10,500	-34	-27	-17	-9	-12	-10	-7	-1
Nose	329	-8	-5	0	0	0	0	0	0
Aft	329	-10	-8	0	0	0	0	0	0
Ramp	496	-10	-8	-5	0	0	0	0	0
Door	496	-9	-7	-4	0	0	0	0	0

[a]Based on Maidanik, reference (15), except where noted.

[b]Based on shaker vibration tests.

TABLE 4

Internal Radiated Sound Power Level[a]
(dB re 10^{-12} Watt)

Panel	S, Area Ft^2	10 log S	Octave Band Center Frequency, Hz							
			63	125	250	500	1K	2K	4K	8K
Bottom	38.0	15.8	105	108	106	106	98	94	83	73
Deck (1)	13.0	11.0	99	108	107	103	90	91	84	70
Lower Side	25.4	14.0	107	110	107	103	98	98	86	76
Sponsons	28.4	14.5	99	102	97	104	100	100	90	77
Upper Side	61.0	17.9	105	113	113	107	97	95	84	72
Top	70.0	18.5	106	113	112	108	98	95	84	72
Bulkhead	14.5	11.6	89	93	96	92	85	94	86	78
Access Panels	14.5	11.6	94	99	101	99	89	89	76	61
Fuel Tank Cover	11.0	10.4	83	95	98	98	83	75	68	68
Nose	11.0	10.4	95	98	112	100	90	87	76	67
Aft	35.0	15.4	96	107	112	103	96	85	80	71
Ramp	13.3	11.2	96	93	97	95	85	81	72	68
Door	6.7	8.3	94	93	90	89	77	72	60	54
TOTAL			113	119	119	114	106	105	95	84

[a]$PWL = AL + 10 \log \sigma + 10 \log S - 20 \log f + 139.7$.

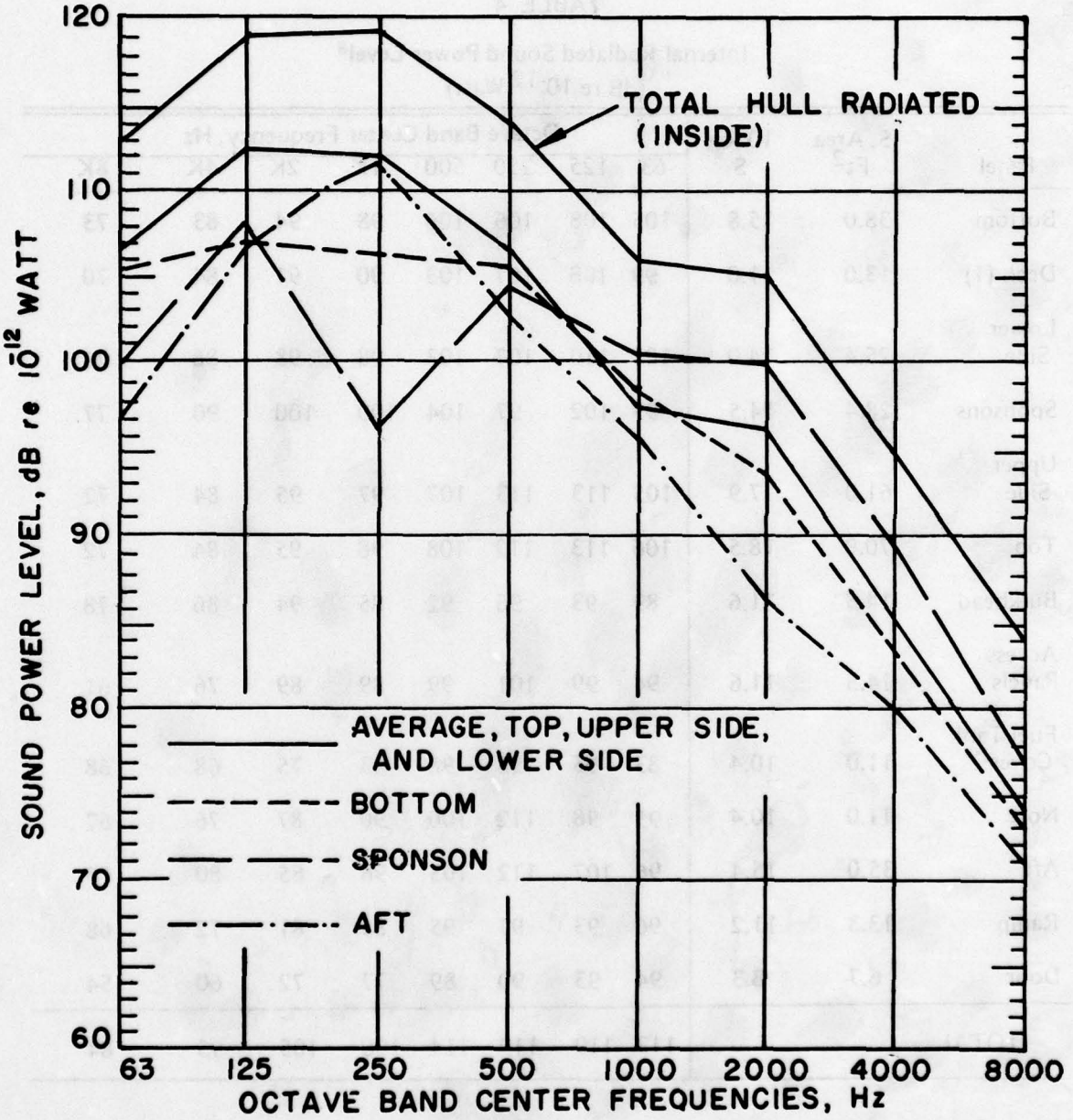

Figure 9. Contributions of individual panels to hull radiated power, baseline vehicle at 20 MPH, vehicle self-powered while supported on jackstands.

radiated power due to their large combined area. Therefore, the use of barriers for effective noise control would require virtually total interior coverage and is therefore an impractical noise control technique. Reference 20 gives results of a complete M113A1 barrier treatment.

Damping Results

Sponson Damping

The lightest structural hull member, the sponson, should theoretically radiate well at high frequencies; however, it does not radiate well in the critical 250 and 500 Hz bands. Nevertheless, the sponson was chosen for damping treatment because of excellent coupling to the rest of the hull and because it forms an energy path from the roadarm suspension mountings to the upper structure. The results of bonding a 5/8" thick layer of damping tile to the sponson are presented in Figure 10. Comparison with Figure 9 shows that not only the sponson, but adjacent plates are also reduced in acceleration levels and radiated power.

The effectiveness of sponson damping was evaluated three ways: from differences in interior noise while running on jackstands, from differences in calculated panel radiation, and by the ratio of hull loss factor with and without damping. The results of these three comparisons are shown in Figure 11. The results are similar, contributing confidence to the experimental results, especially in the 250 and 500 Hz octave bands.

The apparent 6 dB improvement at 125 Hz determined from calculated hull radiation is clearly suspect. The damping material, when tested separately, does not exhibit the loss factor improvement necessary. The apparent improvement is attributed to differences in vehicle track excitation on the tests before and after damping. This obvious error emphasizes the need for evaluating the effect of damping in more than one manner, such as was done above.

Bulkhead and Access Panel Damping

Subsequent to the evaluation of sponson damping, damping materials were applied to the engine compartment bulkhead and access panels. After installation, the treatment was verified to be effective in reducing the vibration levels of those panels. The vehicle with both sponson and access panel damping treatments was then road tested; but no measurable noise reduction was achieved. This contradictory result was attributed to differences between road testing and static operation with the vehicle on jackstands.

Summary of Hull Damping

Additional test track variable speed noise surveys were performed on the vehicle with damped sponsons. The results did not evidence the noise reduction indicated in Figure 11. This result prompted a review of previous and current data which lead to the following conclusions relative to hull damping:

- Test track testing does not produce exactly repeatable noise levels. The variation in force levels was estimated as ± 3 dB in octave bands by comparing available baseline data on a number of different vehicles. For a given vehicle, the variation is less. FMC data suggests ± 2 dB(A) and ± 2 dB(C), and slightly more for octave band data.

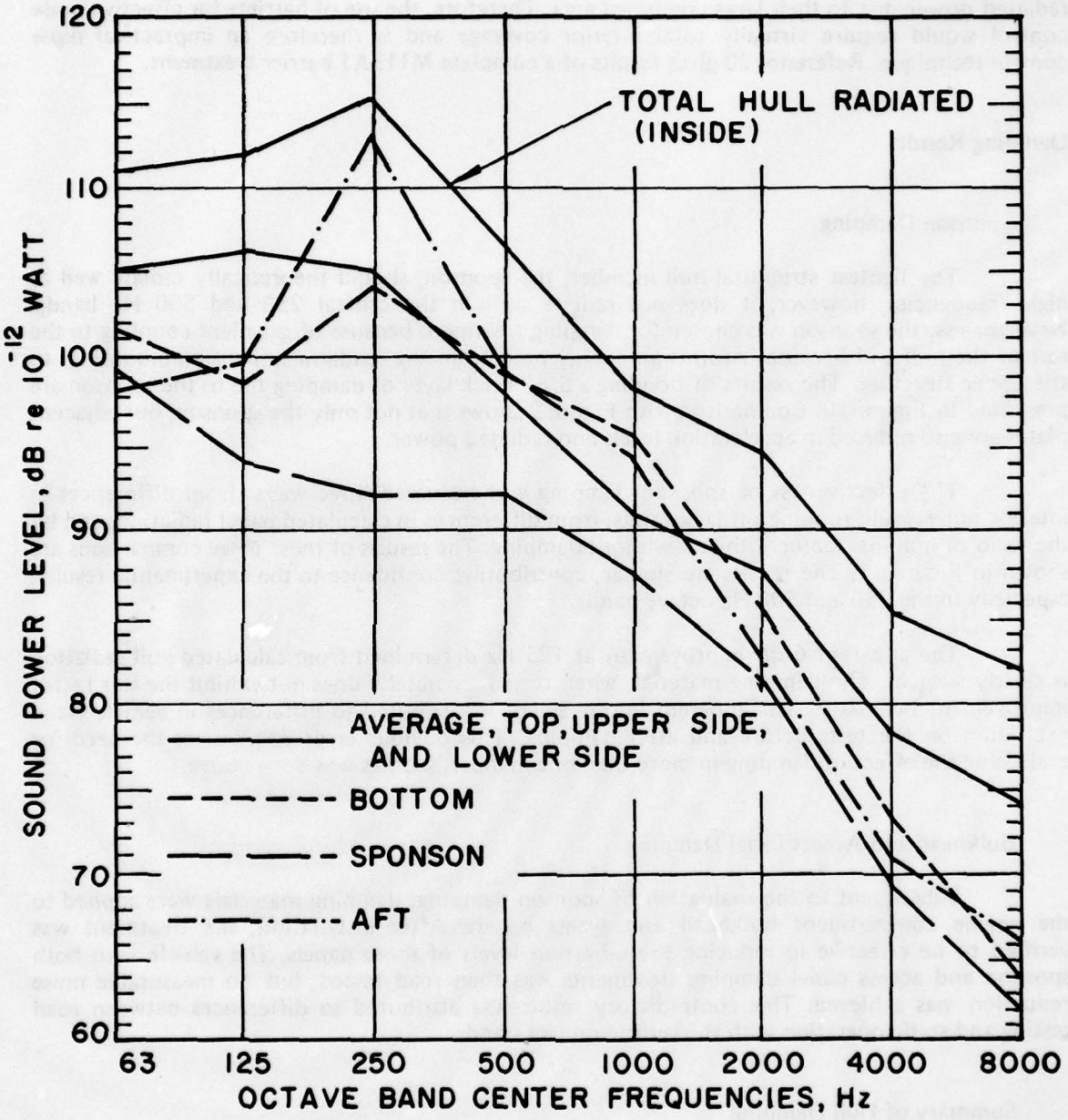

Figure 10. Contributions of individual panels to hull radiated power, damped sponson, 20 MPH, vehicle self-powered while supported on jackstands.

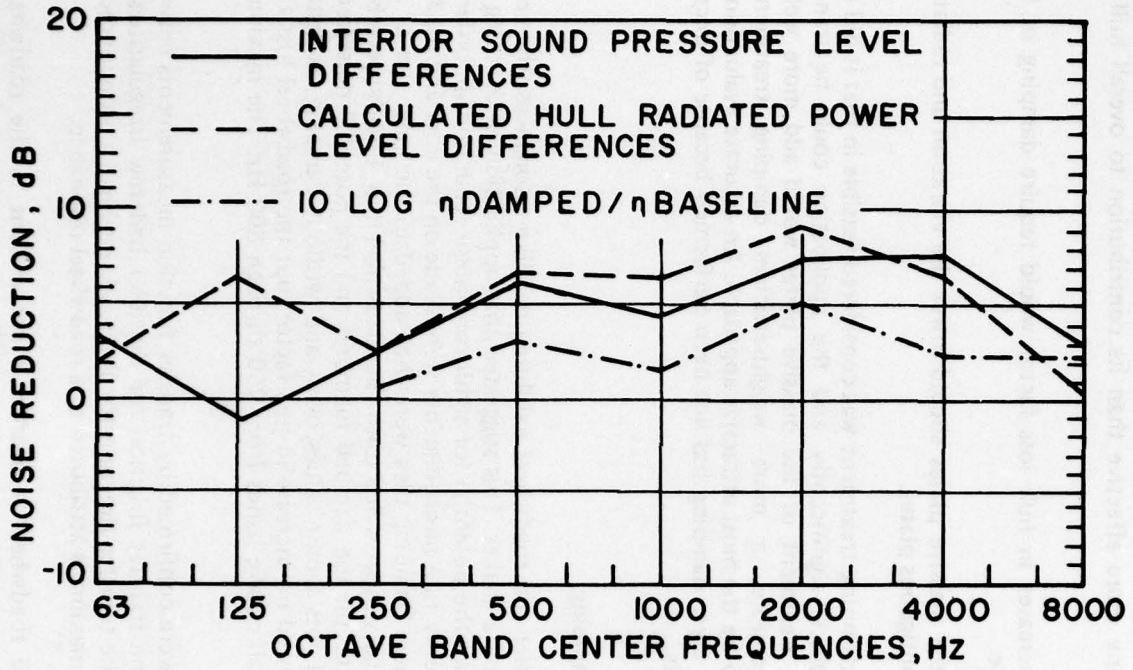

Figure 11. Interior noise reductions due to sponson damping evaluated by three different methods.

- A dip in the noise versus speed curves occurs at 20 mph, usually with high track tension, Figures 6 and 12. This singularity at 20 mph increased the uncertainty in the test results.

- Subsequent evaluation of hull noise reduction measures should be performed with both a controlled force excitation, as well as by test track data.

- Vibratory energy was apparently transmitted to the upper hull via flanking paths around the sponson. In addition, the sponson is not a major source of radiated noise. Therefore, sponson damping was not any more effective than its contribution to overall hull loss factor increase.

- Significant increases in hull loss factor would require damping of the massive plates, especially the top plate.

- Damping of the massive plates should lower the vibration and radiated noise of both the treated plate and contiguous plates.

- The sponson damping treatment was considered feasible in that it did not degrade the performance of the vehicle significantly and the application could be translated to a production process. Similar treatment of the massive plates would add more weight than is considered acceptable. Therefore, a more weight-efficient damping treatment, namely, constrained layer, appears to be the most attractive approach. An accurate evaluation of the cost effectiveness of constrained layer damping has not been performed because of uncertainties in production methods and costs.

Idler and Roadwheel Damping

The unmounted idler and roadwheel exhibited bell-like resonances when either struck with a hammer or excited by a shaker. This suggested that application of damping material to these suspension members had the potential for significant noise reduction. In order to evaluate this potential, reverberant decay rate measurements were made on the idler and roadwheel, with and without the track in place. Damping tiles were then added to the inner rim of an idler and cure-in-place damping material was troweled onto the roadwheel hub. Finally, reverberant decay rate measurements were made on the damped members and the potential noise reduction was calculated from the ratio of loss factor values, with and without damping, as installed with a track in place. The idler showed no increase in loss factor, but the roadwheel loss factor values were more than doubled in all octave bands from 250 through 800 Hz. The maximum increase was 8.5 dB at 250 Hz.

These tendencies were confirmed by transfer function measurements between interior noise and force applied. The transfer function for the idler had few irregularities, increasing gradually with frequency. The transfer function for the roadwheel had a pronounced maxima at approximately 250 Hz. This maxima is attributed to a roadwheel resonance.

The 250 Hz band roadwheel resonance is not evident in the roadwheel noise or roadarm vibration spectra of the preceding HEL-sponsored study. Therefore, the roadwheel-track interaction may already provide significant damping, or resonances of the mounted roadwheels may not be excited to a significant degree during vehicle operation.

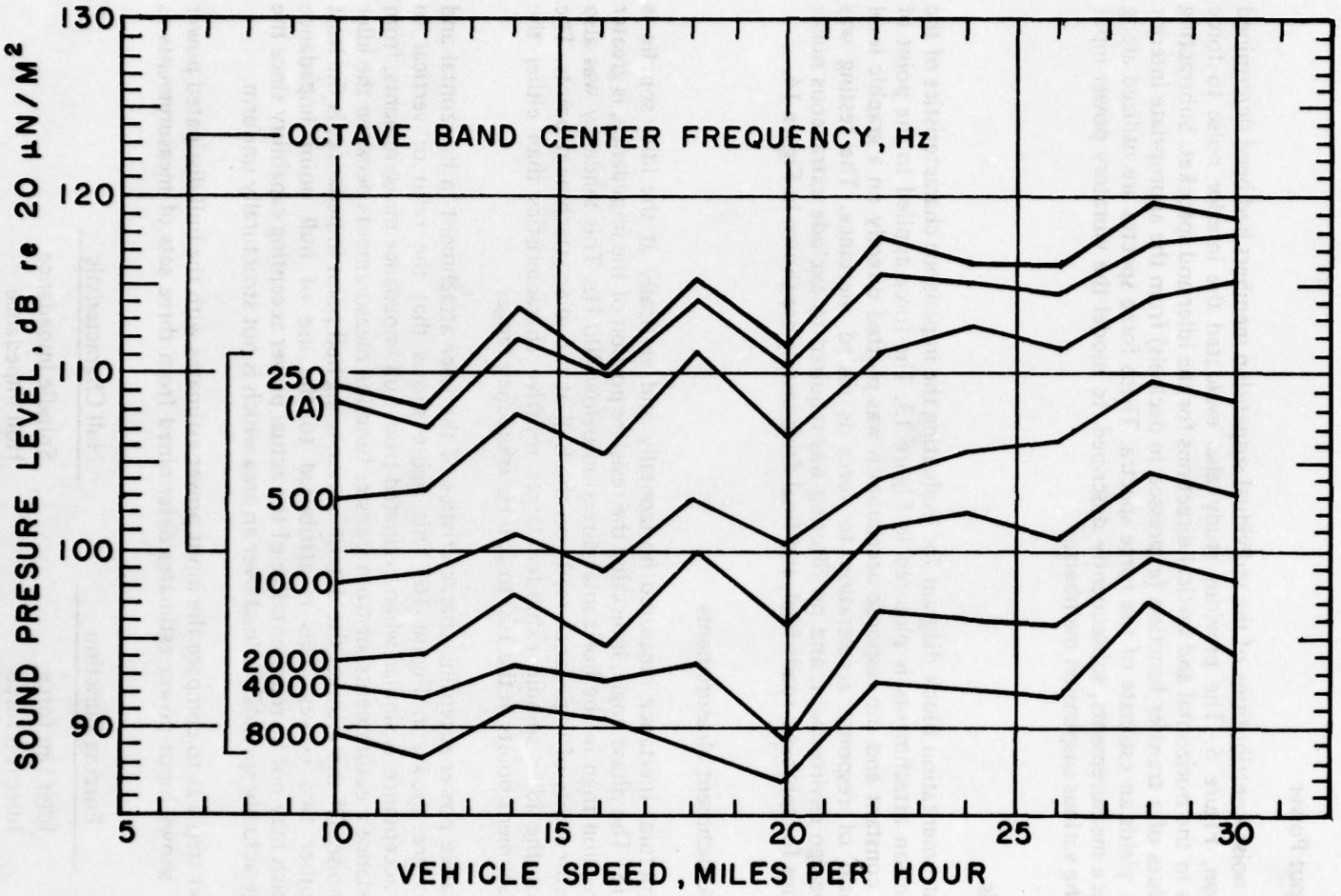

Figure 12. Speed dependence of production M113A1 noise at crew position with damped sponson, bulkhead and panels, vehicle self-powered and supported on jackstands.

In conclusions, the potential for noise reduction using roadwheel damping has been tentatively demonstrated. However, this benefit can only be verified by damping a complete set of roadwheels and repeating the roadwheel tests of Phase I.

Hull Vibratory Input Power

The interior noise contributions of the individual suspension members had been determined by source isolation, Figure 5. The previous study also evaluated the interior noise to force transfer functions in the horizontal and vertical directions for the idler and sprocket. Subtracting the magnitude values of a transfer function (expressed in decibels) from the appropriate interior noise level values yields an estimate of the force spectra. These force spectra are utilized along with the impedance measurements, subsequently described, to model the vibratory power input to the hull from the various suspension members.

Test Methods

The instrumentation block diagram for evaluating the impedance characteristics of the hull at the suspension attachments is pictured in Figure 13. The force applied to the point of interest was held constant and the response acceleration was plotted directly on a graphic level recorder. The ratio of response acceleration to force is called inertance. The testing was performed in a benign environment, and no filtering was required to exclude extraneous noise. Experimental setups for sprocket, roadwheel, and final drive testing are shown in Figure 14.

Suspension Attachment Measurements

The structural inertance measured horizontally and vertically at the idler spindle is shown in Figure 15. The phase angle, indicating the resistive portion of the impedance, is greater in the vertical direction than in the horizontal direction below 400 Hz. This tendency was also evidenced in measurements of impedance made on the hull at the idler attachment points. The top attachment of the idler spindle exhibited larger resistive characteristics than either the forward or aft attachment points in the 100 to 250 Hz frequency range.

The relative power-accepting characteristics of the idler attachment in horizontal and vertical directions are shown in Figure 16. This figure shows that the ratio of vertical to horizontal power acceptance is similar when evaluated from hull impedance measurements, from idler spindle impedance measurements, or from transfer function measurements between the idler rim and interior noise. Of these three, the determination using hull point impedances is the least similar to the other two curves. This is attributed to the use of hull point impedance measurements which may not be representative of the actual power accepting capability since the idler spindle flange actually spreads the load over an area which is not structurally uniform.

The next step was to compare the input power estimates with the hull dissipated power values. Figure 17 shows input power estimates determined from three sets of measurements as follows:

Forcing Function	Hull Characteristic
Idler rim force	Spindle impedance
Idler rim force	Hull impedance
Idler arm acceleration	Spindle impedance

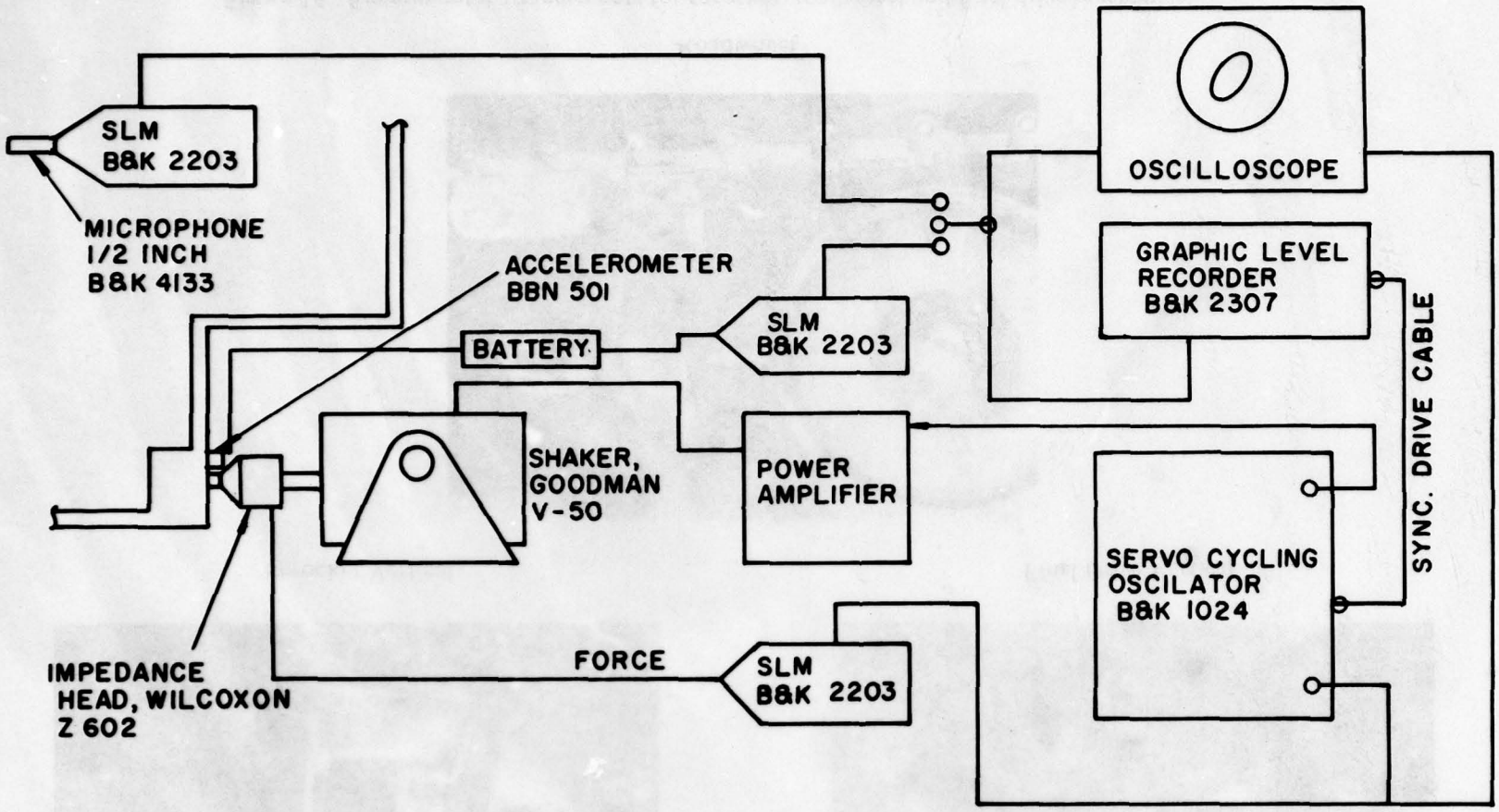

Figure 13. Impedance and transfer function measurement instrumentation block diagram.

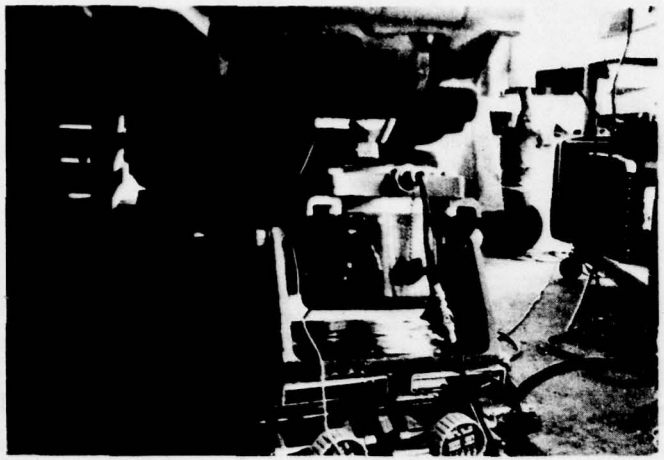

Sprocket Vertical

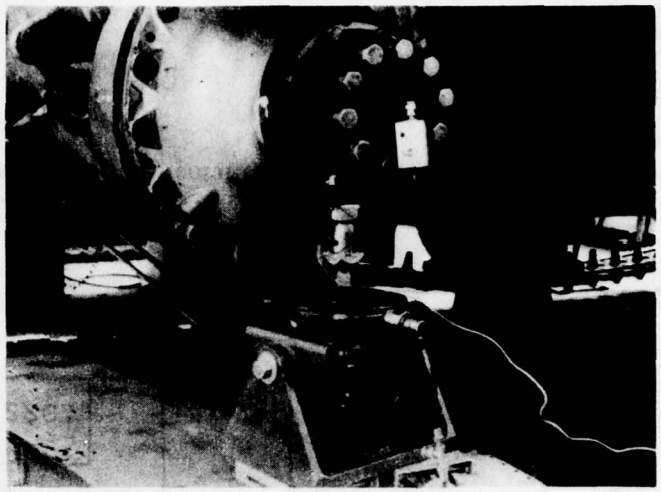

Final Drive Vertical

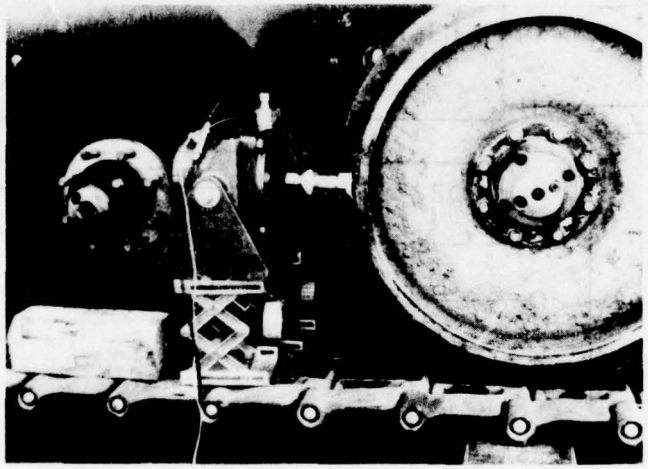

Roadwheel

Figure 14. Experimental arrangements for sprocket, roadwheel and final drive mechanical impedance measurements.

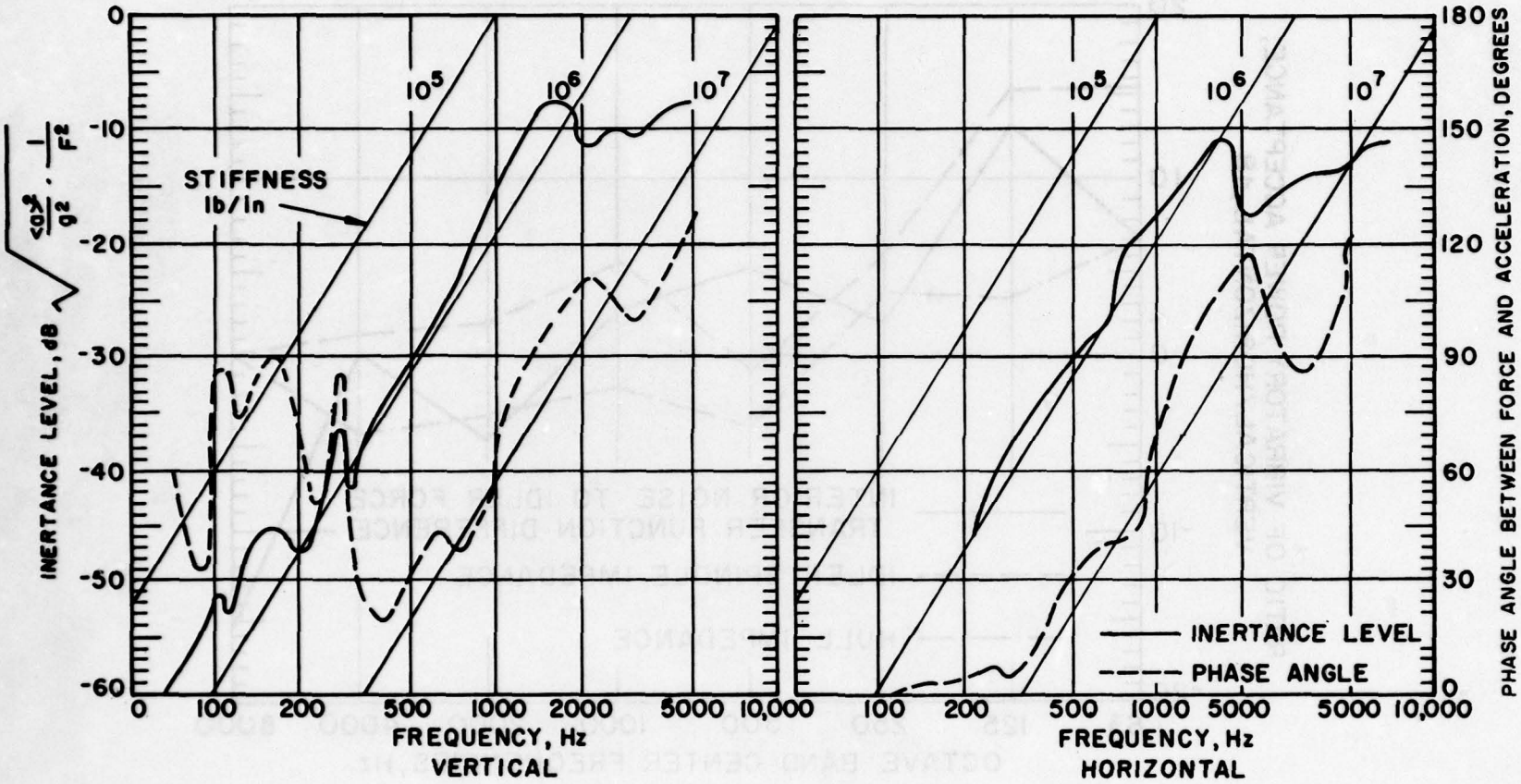

Figure 15. Acceleration response of idler spindle to constant force input, vertical and horizontal directions.

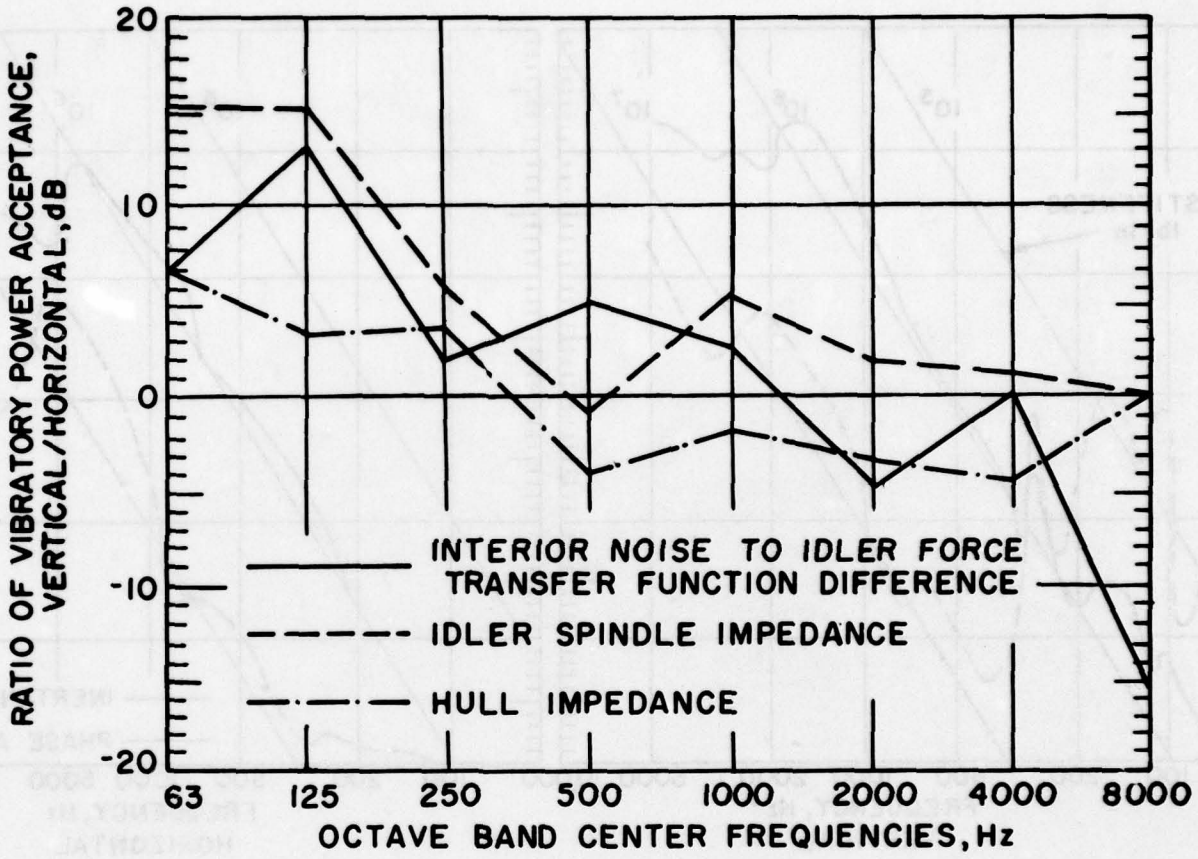

Figure 16. Comparison of idler vertical and horizontal vibratory power acceptance characteristics.

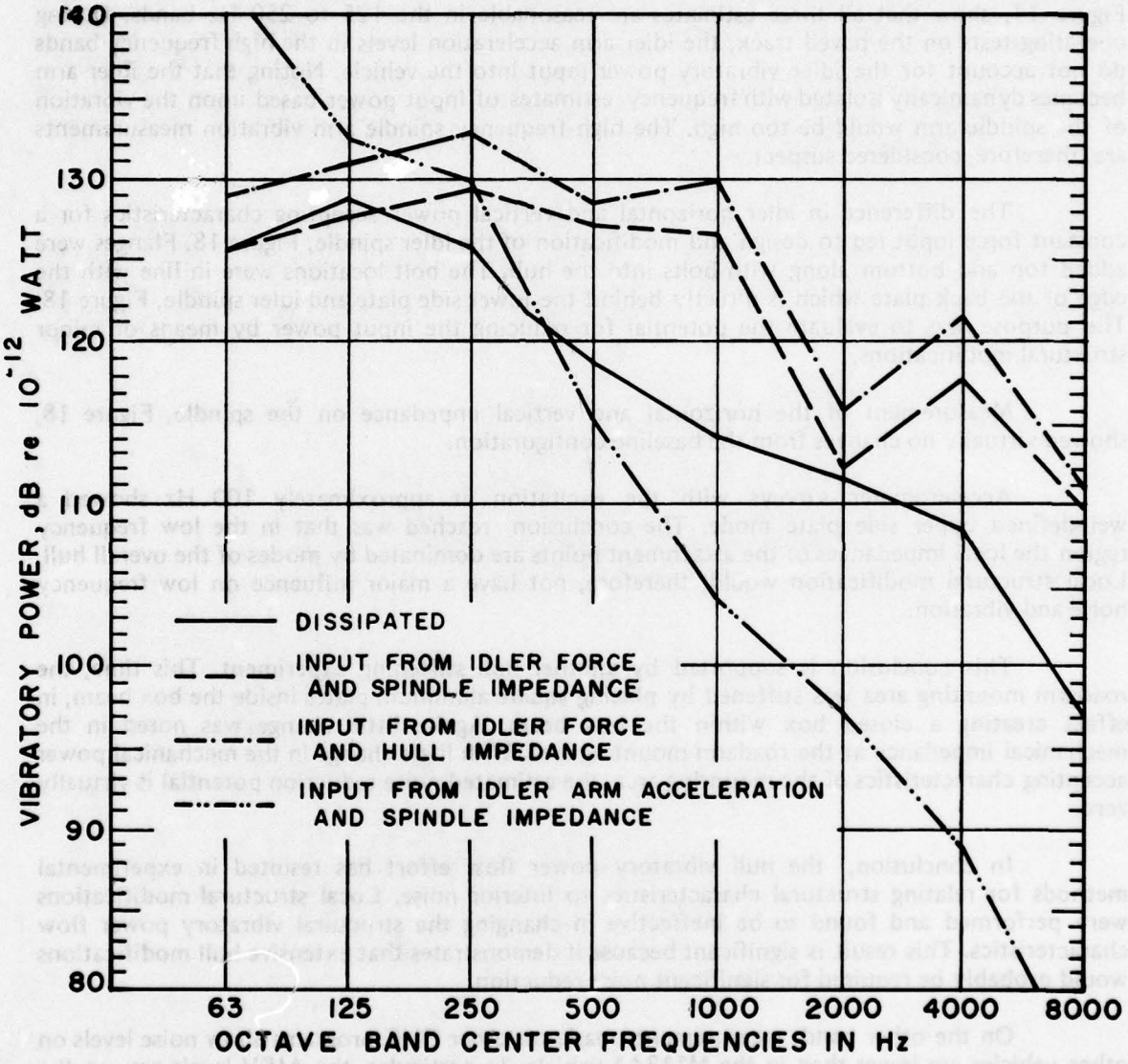

Figure 17. Comparison of calculated input power and hull vibratory dissipated power for idlers.

Note that none of the forcing functions are applied to the same place that the impedance values are measured. This would not be significant in the input force analysis if the idler were a massless spring at all frequencies. However, knowledge of relationships between forces and hull responses is necessary for hull modification and some inaccuracies, if identified, are tolerable. The results, Figure 17, show that all three estimates are reasonable in the 125 to 250 Hz bands. During operating tests on the paved track, the idler arm acceleration levels in the high frequency bands do not account for the idler vibratory power input into the vehicle. Noting that the idler arm becomes dynamically isolated with frequency, estimates of input power based upon the vibration of the spindle arm would be too high. The high frequency spindle arm vibration measurements are, therefore, considered suspect.

The difference in idler horizontal and vertical power accepting characteristics for a constant force input led to design and modification of the idler spindle, Figure 18. Flanges were added top and bottom along with bolts into the hull. The bolt locations were in line with the edge of the back plate which is directly behind the lower side plate and idler spindle, Figure 18. The purpose was to evaluate the potential for reducing the input power by means of minor structural modifications.

Measurement of the horizontal and vertical impedance on the spindle, Figure 18, showed virtually no changes from the baseline configuration.

Accelerometer surveys with the excitation at approximately 100 Hz showed a well-defined upper side plate mode. The conclusion reached was that in the low frequency region the local impedances of the attachment points are dominated by modes of the overall hull. Local structural modification would, therefore, not have a major influence on low frequency noise and vibration.

This conclusion is supported by another hull stiffening experiment. This time, the roadarm mounting area was stiffened by placing square aluminum plates inside the box beam, in effect creating a closed box within the box beam. Again, little change was noted in the mechanical impedance at the roadarm mounting area. With little change in the mechanical power accepting characteristics of the mounting area, the estimated noise reduction potential is virtually zero.

In conclusion, the hull vibratory power flow effort has resulted in experimental methods for relating structural characteristics to interior noise. Local structural modifications were performed and found to be ineffective in changing the structural vibratory power flow characteristics. This result is significant because it demonstrates that extensive hull modifications would probably be required for significant noise reduction.

On the other hand, measurements made on other FMC programs show noise levels on other vehicles are lower than in the M113A1 vehicle. In particular, the AIFV levels are, on the average 4 dB below those of the M113A1 vehicle. This vehicle is different in the method of suspension attachment, the use of space-laminated armor, and an additional sloping plate connecting the upper side plate to the top plate. Any of these differences might account for the lower noise of the AIFV; either of the first two could be adapted to the M113A1 vehicle.

A logical plan for extending the present work involves developing both an analytic and an empirical understanding of the noise characteristics of the hull attachment of various vehicles. This understanding would then form a basis for rational noise control design.

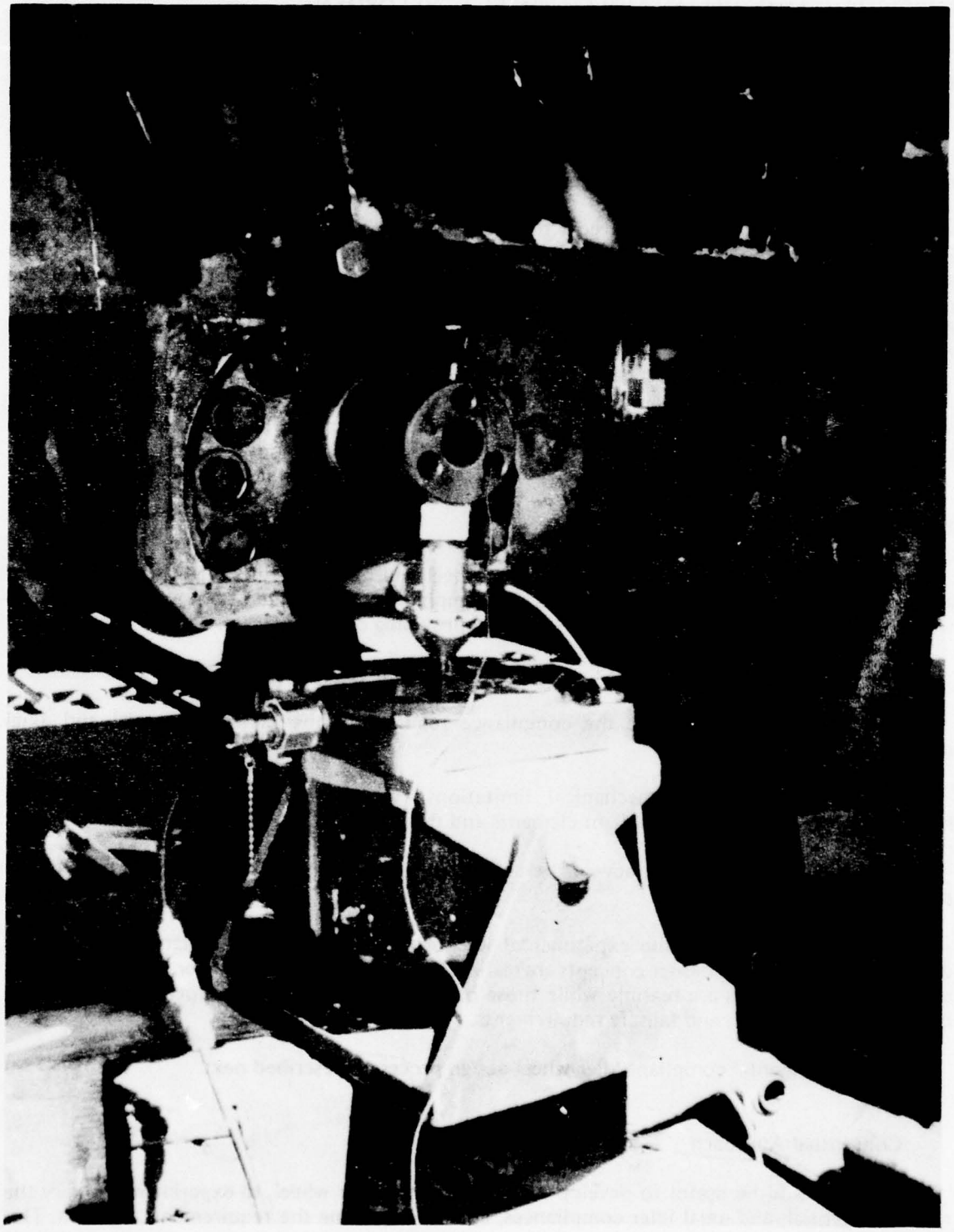

Figure 18. Idler spindle with stiffening tabs and bolts in line with back plate.

EXPERIMENTAL COMPLIANT IDLER WHEEL DEVELOPMENT

Background

In earlier work, it had been shown that an idler or sprocket wheel would generate less interior noise if the wheel rim compliance was increased, that is, if the wheel had a "spring-like" rim, such as could be made with rubber or steel springs (1, 16, 17).

To reach the noise reduction goal of 100 dB(A) for the vehicle, the noise caused by one idler wheel should not exceed 93 dB(A). For the idler wheel, this is a 17 dB(A) reduction at 30 mph (16). To achieve this large amount of noise reduction using a compliant rimmed wheel, the results of Reference 16 (Figure 43), indicate that the radial stiffness should be lowered from 60,000 to below 5,000 pounds per inch. Achieving such a low stiffness will be a considerable challenge in a practical design.

The following sections describe the concepts and design process of an experimental idler wheel. This wheel is the first step in developing a practical, rugged, low noise idler that can be tested on a moving vehicle.

Idler Wheel Design

A practical "production" compliant idler wheel will have difficult weight, cost, durability and noise reduction requirements. Because the compliant rim would add both weight and cost to the vehicle, the idler must not be overdesigned by providing excess softness.

The purposes of designing and fabricating the experimental idler wheel are:

1. To help determine the compliance required in the radial, tangential and axial directions.

2. To check for mechanical limitations and unforeseen failure modes, such as heat-induced failures of the compliant elements and their adhesive bonds.

3. To verify the accuracy of the computer model in predicting noise reductions of the compliant idler.

An inherent benefit of the experimental idler wheel is that, in the design process, it was discovered which basic design concepts are realizeable and which are not. For example, designs utilizing rubber springs are feasible while those based on steel coil springs appeared less practical because of size, weight, and failsafe requirements.

The experimental compliant idler wheel design process is described next.

Conceptual Approach

It would be useful to develop an experimental idler wheel, to experimentally vary the radial, tangential, and axial idler compliances, and to determine the requirements for each. This versatility dictated the use of elastomeric (rubber) springs, as steel and pneumatic springs did not have adequate design flexibility. Also, the expected weight and size of the rubber would be lower than equivalent steel springs.

Practical and mechanical design constraints are that:

1. The idler wheel diameter must be not over 2 inches larger than the present idler to allow the track to be accidentally "thrown." With a larger diameter idler, the track could become jammed between the idler wheel and the sponson, which could cause idler mount or hull failure.

2. The idler springs should be replaceable, both for field practicality in a prototype idler and for ease of experimentation with the present test wheel.

3. For both a prototype and experimental idler, a spring failure should not adversely affect the track operation, although noise could be increased.

4. The experimental design concept should be adaptable to a rugged prototype capable of ingesting debris and withstanding other abusive field conditions, such as bottoming the idler against the ground.

5. It would be desirable, though not mandatory, if the idler would stay registered with the track, as is the case with the sprocket. This registration would allow the use of a specially contoured idler rim which may be advantageous.

6. The prototype design should have a projected life of at least 4,000 miles.

Rubber Spring Design

Preliminary calculations suggested that overheating of the elastomeric springs could be a serious problem. This possibility was supported by a history of heat-induced rubber failures reported in the literature (10, 17, 21, 22, 25) and in discussions with engineers at the U.S. Army Tank-Automotive Research and Development Command (TARADCOM) and FMC. Therefore, a number of rubber compounds were evaluated to identify those with low hysteresis. Low hardness, high-quality, natural-type rubber was selected as having the best combination of high strength and low damping. A further advantage of this choice is the highly developed technology of using natural rubber at large deflections.

The above-mentioned screening of rubber-like materials is described next. First, a number of elastomeric compounds were selected as promising, based on low hysteresis. Next, samples of these compounds were obtained and prepared for testing. The test specimen descriptions and results follow:

1. The first two were medium softness natural rubber of high mechanical properties, specifically Lord Corporation compounds MAH-005 (approximately 45 durometer) and MAH-009 (a little harder at approximately 55 durometer). At below 200 Hz, the loss factor was at or below .08 for the 55 durometer sample and .07 for the 45 durometer sample. The 45 durometer compound had the best combination of mechanical and damping properties of all materials tested.

2. An "economy" natural rubber with extenders was supplied by another manufacturer. At a loss factor of .15, this material was found to have too much hysteresis, so was rejected.

3. Two-wound filament, natural-rubber golf balls (Wilson "Pro-Staff" and Dunlop "Maxfli") were tested with and without the covers. Golf balls were selected because the manufacturers have extensively researched elastomers to achieve low hysteresis. With the covers removed, the hysteresis loss factor was .075 or lower at up to 1400 Hz. However, this material would be expensive, difficult to utilize in practical shapes, and would be subject to chemical attack by lubricants.

4. Two solid golf balls (Dunlop "Tuffli" and a "range" ball, maker unknown) were tested. The loss factors were similar, ranging from .060 to .083. These materials were very hard and thus probably of modest energy storage capability without fracture.

5. Several "Superballs" made by the Whamo Manufacturing Company were tested. These had the least damping of all materials tested with a loss factor of .018 maximum. However, the mechanical properties were very low.

Synthetic-base "natural" rubbers were reported by the manufacturers to have slightly less heat buildup and better mechanical properties than natural "natural" rubber tested. However, the rubber compound selected is, for present purposes, satisfactory, so these synthetics were not pursued in this project.

The loss factors were determined by measuring the sharpness of the resonant peaks. This was accomplished by measuring the frequencies at which the specimen's resonant response has decreased by 3 dB compared to its resonant peak. The loss factor is then given by

$$\eta = 2 \frac{f_+ - f_-}{f_+ + f_-}$$

where f_+ is the -3 dB frequency above the resonance, and f_- the -3 dB frequency below the resonance. The formula is only accurate for reasonably sharp resonances, such as in these tests.

The elastomer specimen was mounted on a specially machined impedance head which was mounted on a 1 pound mass which, in turn, was mounted on a Ling 200 series electrodynamic shaker. The frequencies were measured with an electronic counter. The output response signal was from the force transducer in the impedance head.

This "customized" test method was chosen over using a conventional dynamic modulus apparatus as the latter would have required an unavailable specimen shape.

The test method utilized only small strains of the material samples, typically 1 percent or less. Since in actual use in a compliant idler, the strains may be 25 percent or more, the above tests were only used to screen materials (as opposed to using the data for calculating heat buildups in the idler wheel design). More elaborate testing was required for design purposes, as described next.

Rubber Spring Testing

Even with natural rubber compounds, a moderate heating problem could exist, which would lessen rubber life and increase the infrared signature. Therefore, a sinusoidal cycling experiment was designed to simulate long duration 30 mph vehicle operation on sample rubber spring elements. This test demonstrated that overheating was not a serious problem especially for the softer of the two natural rubber springs tested, and that no evidence of fatigue damage was

evident after 100,000 cycles at a displacement greater than will occur on the experimental idler wheel. Thus, the rubber springs would be durable enough for an experimental idler wheel. A more detailed description of this rubber heat buildup experiment follows:

The test specimens consisted of rubber-in-shear springs made of two 1/2" thick by 2-1/2" x 3" rubber pads, with one pad adhesively bonded to each side of a 1/2" thick aluminum center "paddle." The outer rubber surfaces were then attached to a fixed steel frame thusly forming a five-layered sandwich, as shown on Figure 19. Two rubber samples were tested, one nominally 55 Durometer (Lord Corporation Compound No. MAH-009) and one nominally 45 Durometer (Lord Corporation Compound No. MAH-005). The upper temperature limit of these materials is 220°F; however, the mechanical properties are reduced at that temperature, and it is preferred to not exceed 180°F in the compliant idler wheel design.

During the testing, the center aluminum paddle was attached to a dynamic testing machine actuator, as shown in Figure 20. The resulting motion strained the two rubber pads in shear in one direction. (In actual idler operation, the paddles would experience a relatively complex motion depending upon the position of the track relative to the idler.)

Thermocouples were fastened to the stationary frame centered over the rubber pads and also to the edge of the aluminum center paddle. During the final tests, a thermocouple was also inserted into the center of the rubber pieces to determine the maximum temperature occuring within the compliant element.

During all tests, the sample's heat rejection was <u>not</u> aided by induced air motion, such as with a fan.

Heat and Fatigue Test Results

The rubber tests showed that the softness of the rubber greatly affects the temperature rise. As can be seen in Table 5, at 100 percent shear strain after 30 minutes of cycling at 10 Hz, the increase in temperature of the harder rubber was over 2-1/2 times that of the softer rubber. There are two readily apparent reasons for this. First, the harder rubber accumulates greater potential energy during each cycle. Second, the harder rubber is less resilient, that is, it has more damping.

The temperature at the center of the softer sample after 20 minutes at 10 Hz was 10°F above that of the aluminum center paddle. This strongly suggests that for 1/2-inch thick rubber samples, the center of the rubber will not have a tendency to overheat or "blow out."

To increase the severity of the fatigue test, the rubber was at zero strain at one end of each stroke. This is because, with rubber, any strain cycle that includes zero strain (such as a 0 to 25 percent strain cycle) will normally result in a lower fatigue life than a cycle of identical stroke but not including zero strain (such as a 25 to 50 percent strain cycle).

No evidence of fatigue damage was found in either rubber sample after all tests were complete. The most severe of these tests consisted of 10^5 sinusoidal cycles of 100 percent maximum strain at 10 Hz, which simulated 95 miles of 30-mph vehicle operation. Based on these tests, it was concluded that the rubber spring configuration is suitable for use in the experimental compliant idler wheel.

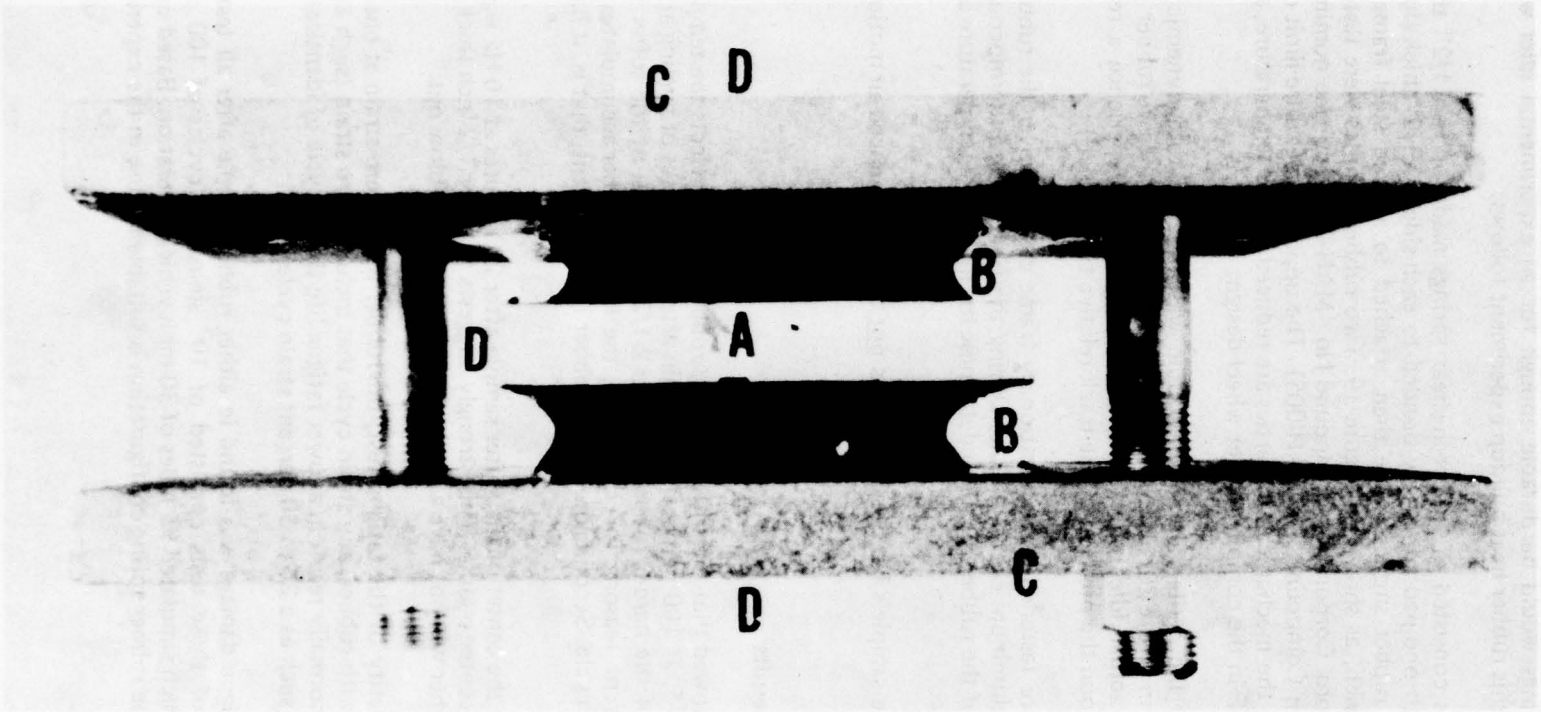

The letters indicate the following: (A) aluminum plate, (B) rubber samples, (C) steel plate, and (D) thermocouples. Force was applied along the axis coming out of the photograph.

Figure 19. Rubber sample test fixture.

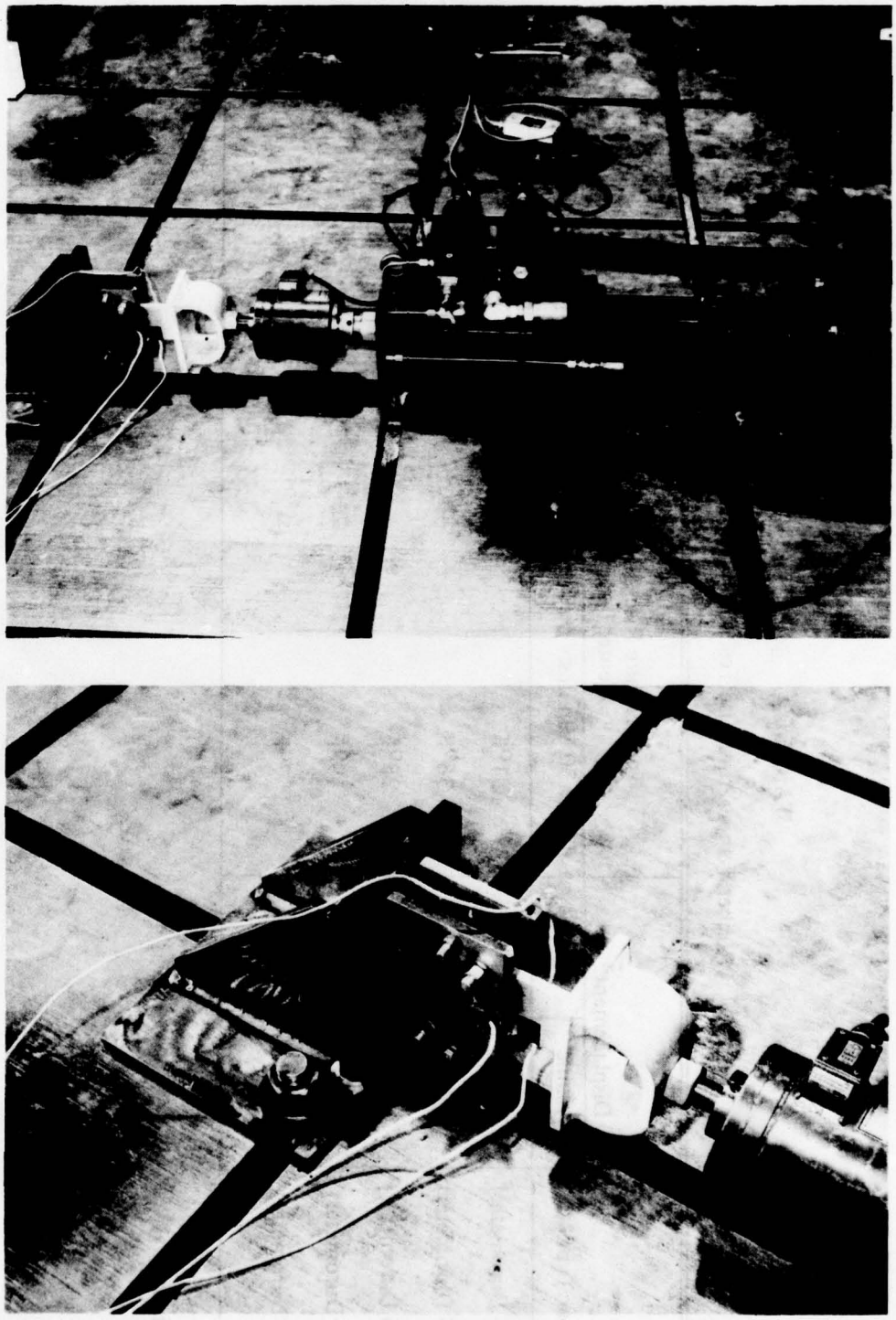

Figure 20. Testing of rubber spring.

TABLE 5

Rubber Temperature Rise Test Results

Rubber Type	Displacement[a]		Temperature Rise Of Aluminum Center Paddle		Temperature Difference Between Center of Rubber and Aluminum Center Paddle After 20 Minutes
	Dynamic	Static	After 30 Minutes	After 216 Minutes	
Hard (55 Durometer)	1/2	1/4	51°F	68°F	–
Hard (55 Durometer)	3/8	5/16	36°F	–	–
Hard (55 Durometer)	1/4	1/8	23°F	–	–
Soft (45 Durometer)	1/2	1/4	19°F	–	10°F
Soft (45 Durometer)	1/4	1/8	7°F	–	–

[a]10 Hz Sinusoidal

The softer compound was chosen for the experimental wheel because it provided both adequate stiffness and appears to have no overheating problems. Results of idler heat rejection test conducted by FMC (8) showed that the idler wheel can, itself, reject large amounts of heat, so it will not become hot but will remain at approximately the same temperature as the standard idler wheel.

Description of Experimental Quiet Idler Wheel

The experimental compliant idler wheel as fabricated is shown on Figures 21, 22 and 23. It is well suited to experimental changes and has a projected useful life in excess of 10^5 revolutions. Installed, it replaces the outer idler wheel half. The track is supported by 11 rubber-in-shear springs which are mounted to a hub assembly. The maximum stroke of the compliant elements is 5/8 inch and the radial spring rate of each paddle is variable from approximately 1,000 to 20,000 pounds per inch through choice of dimensions and rubber characteristics.

The 100,000 cycle fatigue life is satisfactory for an experimental wheel. However, a greater fatigue life would be required for a production idler; for example, 6×10^6 cycles for a 6,000-mile life wheel. A 6,000-mile wheel life is considered feasible by increasing the rubber pad thickness, reducing the stroke, and pre-straining the rubber pads.

Future Idler Noise Reduction Experiments

Sound level measurements will be made in the vehicle interior by mounting the experimental idler wheel to a stationary vehicle. This vehicle will be supported on blocks with the tracks not touching the ground. The sprocket will be attached to a separate test stand to ensure that sprocket noise does not influence the idler noise measurement. This test stand arrangement is more fully described in Reference 16.

Since only a half-idler is to be tested, it should be questioned as to how well its vehicle interior noise will compare to that of a complete idler pair. The following arguments suggest that no serious problems should exist:

First, the idler half is only half as stiff as the complete pair would be. For this reason, track tension will be adjusted to half its normal value. This should be taken into account when utilizing data.

Second, the track impacts may cause vibration in several directions because of the unbalanced forces. (This is commonly called "coupling" between the modes of vibration.) For example, a vertical track shoe impact would cause idler vibration in all three directions. However, this coupling action has also been shown to occur with the standard idler pair when vibrated with an electrodynamic shaker, and is probably also a normal condition.

A third result of having only a single wheel half is that the track will tend to wander to one side of the idler wheel, which will cause rubbing of the track guide on the idler. This was demonstrated when the experimental idler wheel was installed on the test stand and the track rotated. The rubbing was severe enough to cause appreciable wear of the aluminum idler wheel hub. The anticipated "fixes" will be to install a more wear-resistant contact surface on the idler wheel, to cant the entire idler assembly, and to provide better roadwheel guidance by modification of the test stand.

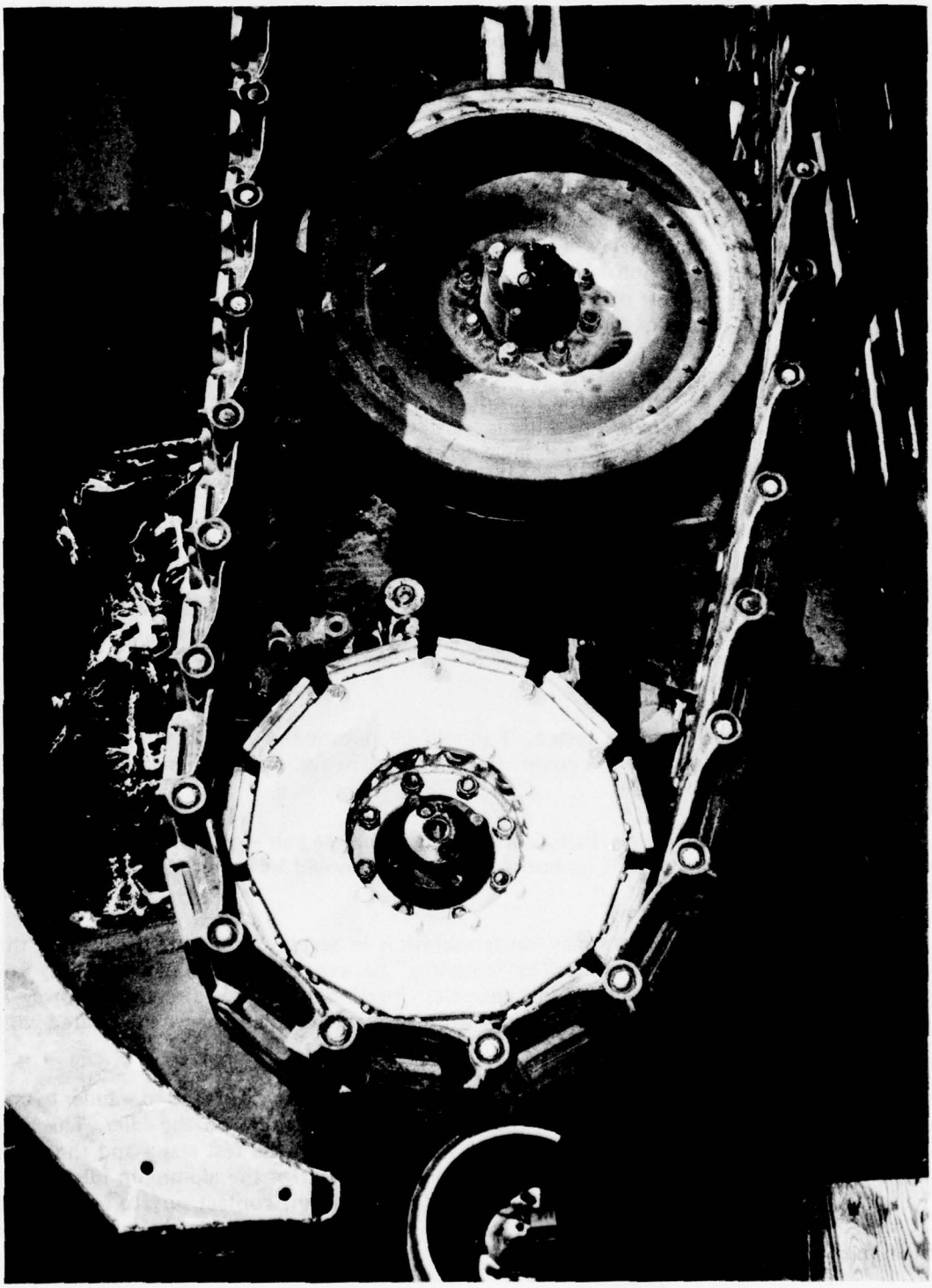

Figure 21. Experimental idler wheel mounted on vehicle.

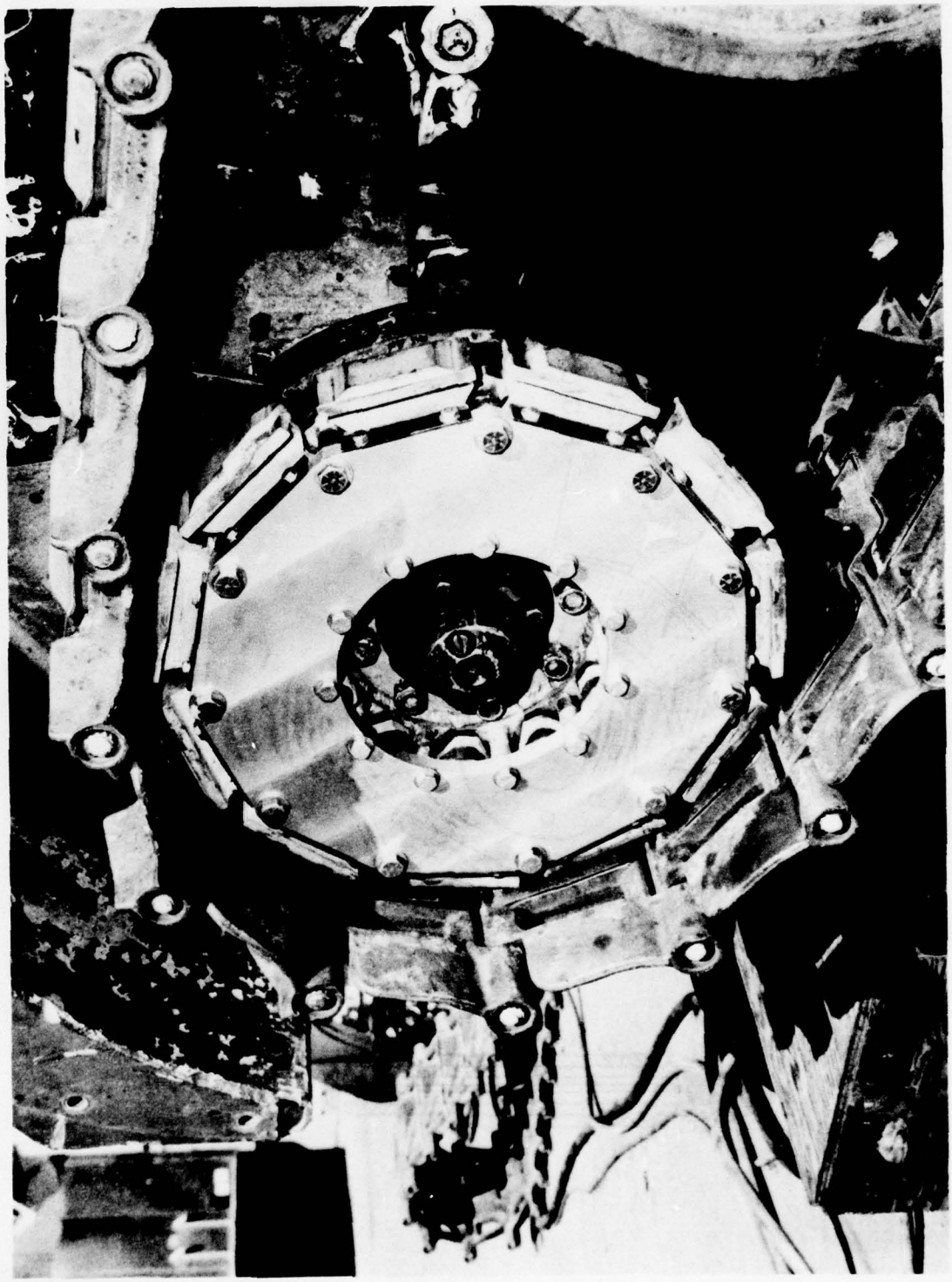

Figure 22. Experimental idler wheel mounted on vehicle (closeup).

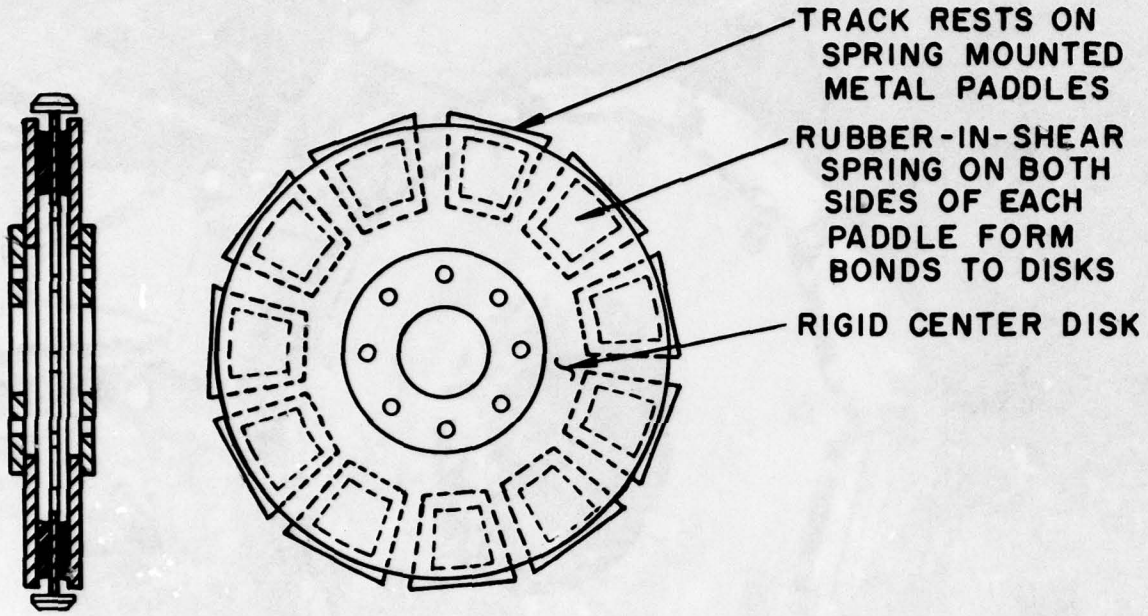

Figure 23. Schematic diagram of experimental idler wheel.

Although the experimental idler wheel was not tested in this program, it was cycled sufficiently to be confident that it was ready for testing. However, this cycling also revealed that the test stand itself may cause high levels of vehicle interior noise which may mask the sound of a low-noise idler wheel. The test stand is now being modified to allow testing of idler wheels which are significantly quieter than those which have been available in the past.

Other Compliant Idler Design Options

The present experimental idler design supports the track on 11 paddle-shaped impact absorbers. This concept is suitable for experimentation. However, other design concepts have been considered that have cost, durability, weight, or other advantages for production. Those seriously discussed in the course of this program include:

1. Supporting the track on a steel hoop, which may or may not be flexible. This hoop would, in turn, be supported on rubber spring(s), as shown in Figure 24. The advantages are that fewer parts are used, less rubber is needed, the rubber would be less heated, and the weight is potentially lower than with other compliant idler designs.

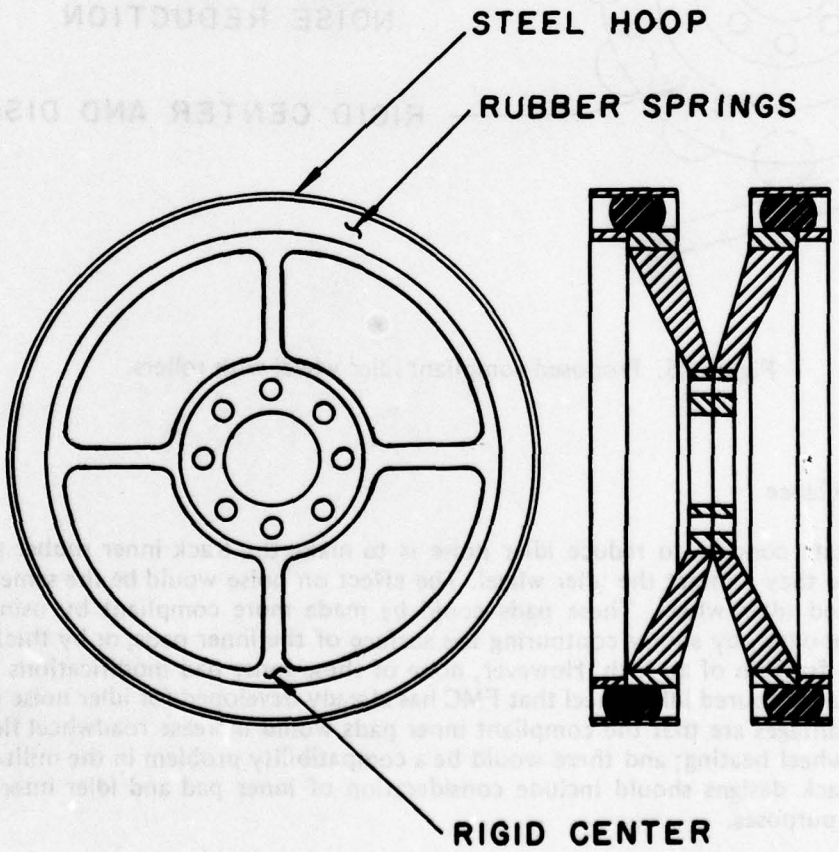

Figure 24. Proposed compliant idler with rubber ring and wear-resistant steel hoop.

2. A design similar to the present experimental idler, except that the impact absorbers would be commercially-available rubber doughnuts that can rotate. Possible advantages are slightly lower vehicle rolling resistance compared to the hoop or standard idler wheel, the components are commercially available, and tangential compliance is provided by the rotating doughnuts. This concept is shown in Figure 25.

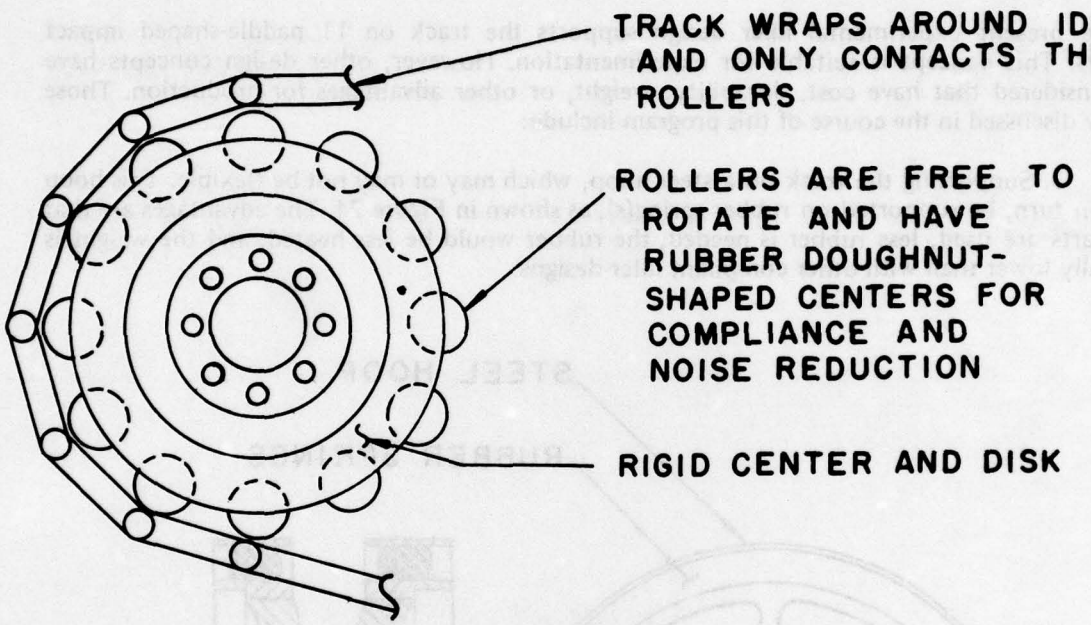

Figure 25. Proposed compliant idler wheel with rollers.

Inner Pad Compliance

One alternate concept to reduce idler noise is to make the track inner rubber pads more compliant where they contact the idler wheel. The effect on noise would be the same as for the compliant-rimmed idler wheel. These pads could be made more compliant by using a softer rubber pad compound, by subtly contouring the surface of the inner pads, or by thickening the pads by a small fraction of an inch. However, none of these inner pad modifications offers any advantage over a contoured idler wheel that FMC has already developed for idler noise reduction. Probable disadvantages are that the compliant inner pads would increase roadwheel flexing and, therefore, roadwheel heating; and there would be a compatibility problem in the military supply system. New track designs should include consideration of inner pad and idler interaction for noise reduction purposes.

TRACKED VEHICLE COMPUTERIZED DYNAMIC ANALYSIS

Introduction

This section of the report describes the purposes and the results of a computerized dynamic analysis of the track idler and sprocket system.

This report is descriptive in nature and does not present the derivation of the equations of motion, nor the actual computer program. More detailed information is in a separate document because of space limitations (6).

The present computer program builds upon previous work for the U.S. Army Human Engineering Laboratory described in Reference 16. The present work includes more parameters and uses more sophisticated analytical techniques to provide a more flexible and realistic description of a real vehicle track system.

Objective

The technical objective of this work is to develop a means of predicting interior noise levels induced by the track and suspension system. This computer program would then be useful in designing compliant idler and sprocket wheels and other track or suspension modifications to reduce noise.

Thus, some costly "cut and try" wheel development could be avoided by screening candidate idler designs and only selecting the most promising for further development.

Another computer program use is to create a data bank of the effect on interior noise due to changing idler and sprocket wheel diameters, wheel radial and tangential stiffnesses, damping, track block length and mass, and track tension. A schematic showing the parameters of the track-wheel system, appears in Figure 26.

Description of Computer Program

The basic operation of the computer program is described next and is shown on Figure 27. In Blocks 1 and 2, the user-supplied parameters mentioned earlier are read by the computer. In Block 3, the track system geometry is initialized by incrementally moving the idler and sprocket wheels apart and allowing the track to stretch into position. All compliances, such as the track bushings and compliant wheel rims, attain their initial strains. This initialization step is necessary to avoid severe start-up transients that would occur with a less elaborate initializing subroutine. In Block 4, the positions of the track links are calculated as the track moves and the wheels rotate. In Block 8, the vibration forces exerted on the idler and sprocket are calculated based on the previously determined track link positions, and in Block 9, the resulting force spectrum in 1/3 octaves is calculated. The force spectra in the vertical and horizontal directions are then converted to 1/3-octave band A-weighted interior noise levels by means of a table of experientially generated force-to-noise transfer functions. The program's output includes tabulated noise spectra and graphical presentations of the force-time history, the plotted noise spectra, and a diagram of the track block positions at selected times.

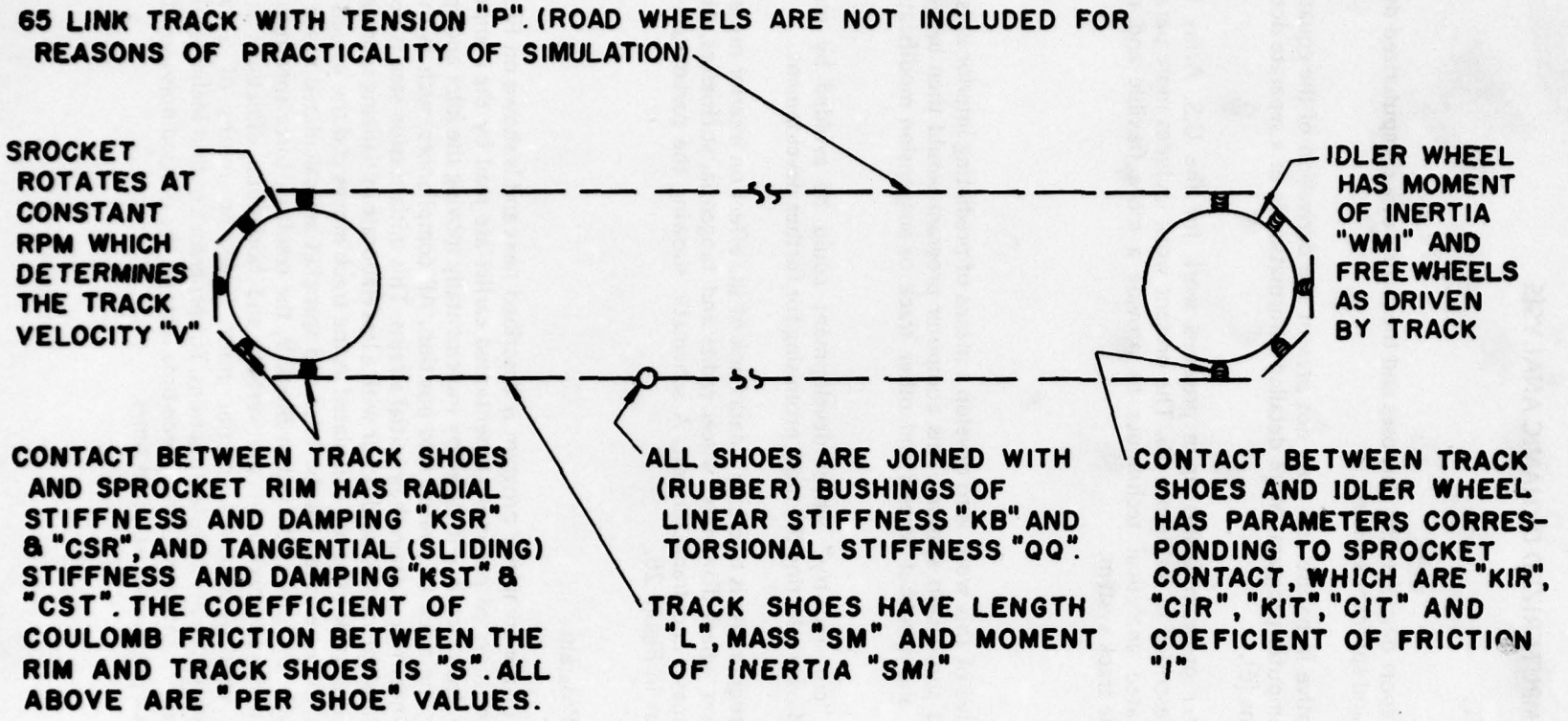

Figure 26. Schematic of track simulation showing the parameters of the track-wheel system.

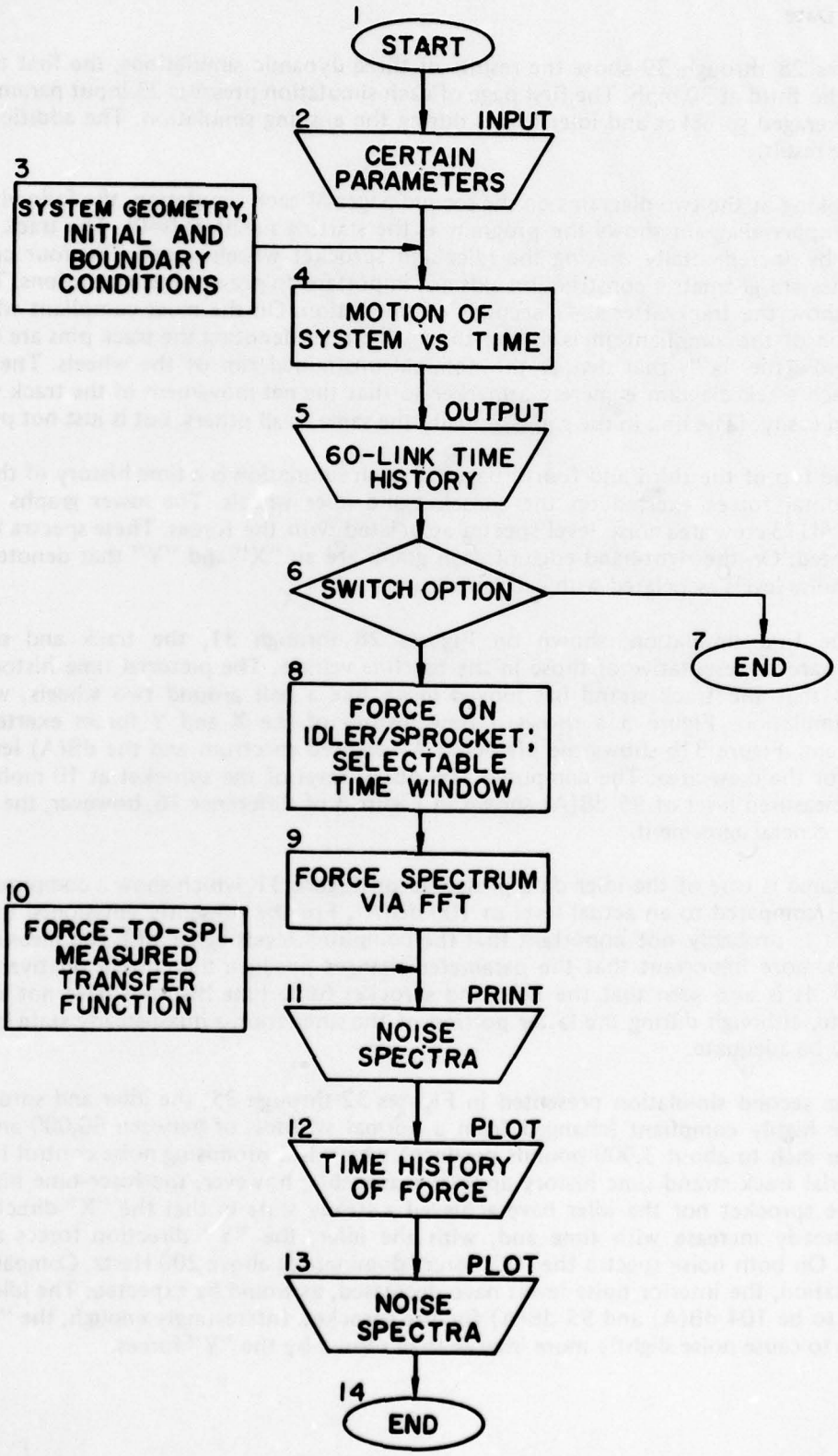

Figure 27. Flow diagram for the Phase II track vehicle computer program.

Results to Date

Figures 28 through 39 show the results of three dynamic simulations, the first two at 10 mph and the third at 30 mph. The first page of each simulation presents 23 input parameters and the time-averaged sprocket and idler forces during the ensuing simulation. The additional pages present the result.

In looking at the two diagrams on the second pages of each simulation, the following can be seen. The upper diagram shows the program at the starting position (t=0). The track has been tensioned by incrementally moving the idler and sprocket wheels apart. The four converging straight lines are geometric construction aids not important to present interpretations. The lower diagrams show the track after 0.41 seconds of simulation. On the most compliant wheels, the compression of the compliant rim is visible—the small circles denoting the track pins are depressed slightly below the "x"'s that denote the nominal unstrained rim of the wheels. The "missing link" in each track diagram is merely a marker so that the net movement of the track with time can be seen easily. (The link in the gap is actually the same as all others, but is just not printed.)

At the top of the third and fourth pages of each simulation is a time history of the vertical and horizontal forces exerted on the sprocket and idler wheels. The lower graphs show the calculated M113 crew area noise level spectra associated with the forces. These spectra have been "A" weighted. On the right-hand edge of each graph are an "X" and "Y" that denote the "A" weighted noise levels associated with each spectrum.

In the first simulation, shown on Figures 28 through 31, the track and suspension parameters are representative of those in the baseline vehicle. The pictorial time history, Figure 29, shows that the track strand has moved much like a belt around two wheels, which is a realistic simulation. Figure 31a shows a time history of the X and Y forces exerted on the sprocket, and Figure 31b shows the predicted A-weighted spectrum and the dB(A) level of the sprocket for the crew area. The computed 105 dB(A) level of the sprocket at 10 mph is higher than the measured level of 95 dB(A) shown in Figure 3 of Reference 16, however, the spectrum shape is in general agreement.

The same is true of the idler data presented on Figure 31, which show a computed level of 112 dB(A) compared to an actual level of 100 dB(A). For the presently envisioned uses of the program, it is probably not important that the computed levels agree with the measured noise levels; it is more important that the parameter changes produce the correct relative change in noise level. It is also seen that the idler and sprocket force time histories have not achieved a steady state, although during the latter portion of the simulation a quasi-steady state is achieved which may be adequate.

In the second simulation presented in Figures 32 through 35, the idler and sprocket rims were made highly compliant (changed from a normal stiffness of between 60,000 and 70,000 pounds per inch to about 3,000 pounds per inch) which is a promising noise control technique. The pictorial track strand time history appears reasonable; however, the force-time histories on neither the sprocket nor the idler have achieved a steady state in that the "X"-direction force shows a steady increase with time and, with the idler, the "Y" direction forces also show transients. On both noise spectra the "X" forces dominate at above 200 Hertz. Compared to the first simulation, the interior noise levels have decreased, as would be expected. The idler noise is predicted to be 104 dB(A) and 95 dB(A) for the sprocket. Interestingly enough, the "X" forces are shown to cause noise slightly more intense than caused by the "Y" forces.

RUN NO. 1

SPROCKET RADIUS	RS	(IN)	= 9.50
IDLER RADIUS	RI	(IN)	= 9.50
TRACK PITCH	L	(IN)	= 6.00
NUMBER OF SHOES	NS		= 65.00
SPROCKET TANGENTIAL STIFFNESS	KST	(KLB/IN)	= 100.00
" DAMPING COEF.	CST	(LB*SEC/IN)	= 37.65
SPROCKET RADIAL STIFFNESS	KSR	(KLB/IN)	= 77.00
" DAMPING COEF.	CSR	(LB*SEC/IN)	= 33.00
IDLER TANGENTIAL STIFFNESS	KIT	(KLB/IN)	= 100.00
" DAMPING COEF.	CIT	(LB*SEC/IN)	= 37.65
IDLER RADIAL STIFFNESS	KIR	(KLB/IN)	= 77.00
" DAMPING COEF.	CIR	(LB*SEC/IN)	= 33.00
BUSHING STIFFNESS	KB	(KLB/IN)	= 140.00
BUSHING DAMPING COEF.	CBL	(LB*SEC/IN)	= 44.54
BUSHING TORSIONAL STIFFNESS	QQ	(KLB*IN/RD)	= 2.24
SPROCKET COULOMB FRICTION COF.	MUS		= .30
IDLER COULOMB FRICTION COF.	MUI		= .30
VEHICLE VELOCITY (MPH)	V	(MPH)	= 10.00
TRACK SHOE MASS	SM	(SLUGS)	= .63
TRACK SHOE MOMENT OF INERTIA	SMI	(SLG*IN**2)	= 1.87
IDLER MOMENT OF INERTIA	WMI	(SLG*IN**2)	= 146.88
TRACK STRAND TENSION	TNS	(KLBS)	= 3.00
TIME-AV. X-FORCE ON SPROCKET	Q1	(KLBS)	= 8.12
TIME-AV. Y-FORCE ON SPROCKET	Q2	(KLBS)	= -.03
TIME-AV. X-FORCE ON IDLER	Q3	(KLBS)	= -8.13
TIME-AV. Y-FORCE ON IDLER	Q4	(KLBS)	= .01
SAMPLING TIME	T0	(MSEC)	= .10

Figure 28. Baseline run, 10 MPH; Input data and time averages of X and Y forces on idler and sprocket wheels.

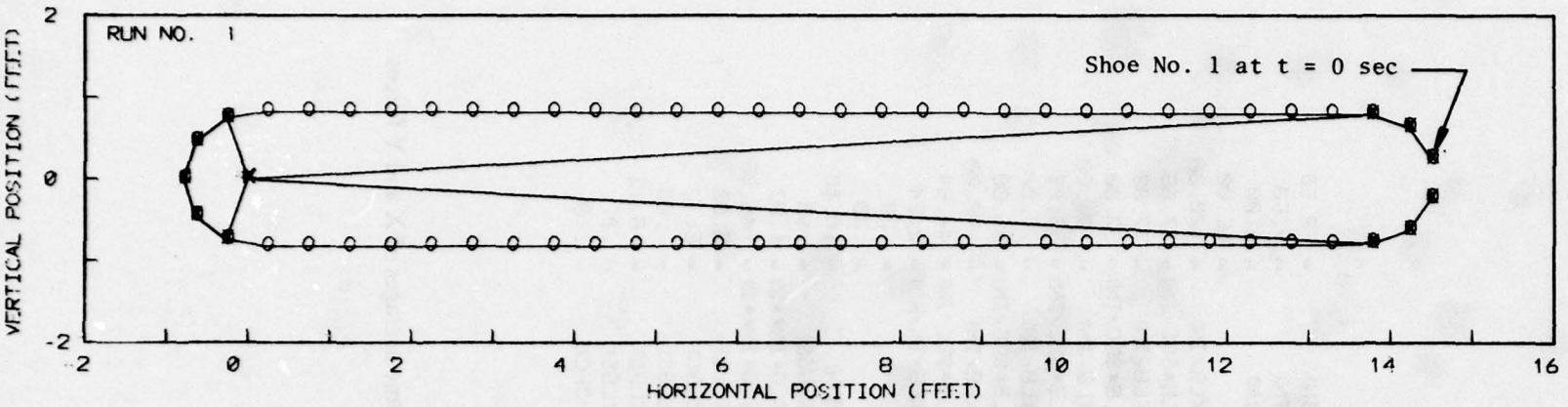

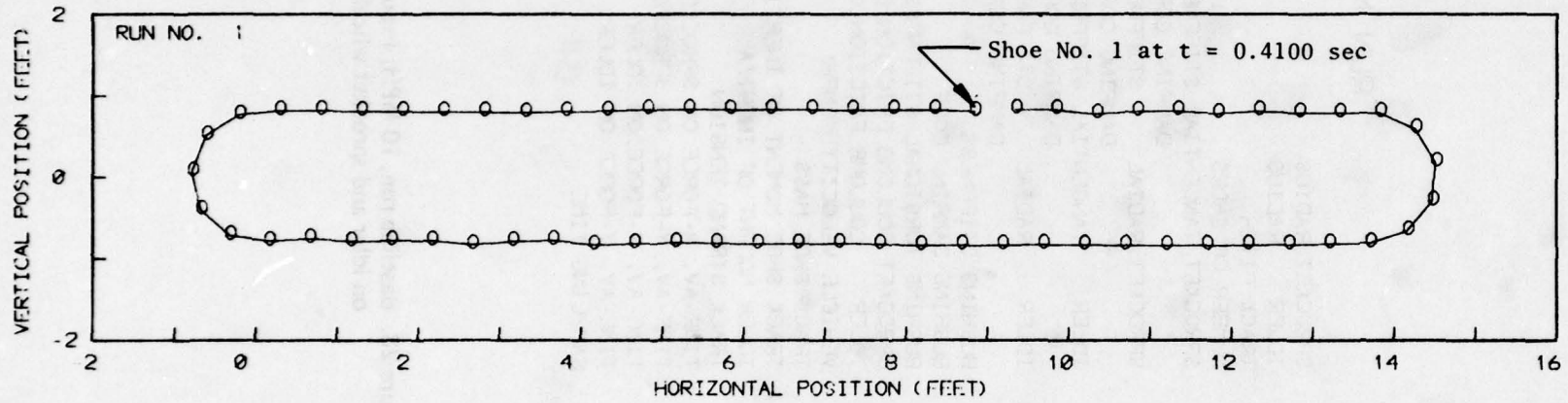

Figure 29. Baseline run, 10 MPH; Diagrams of track shoe positions.

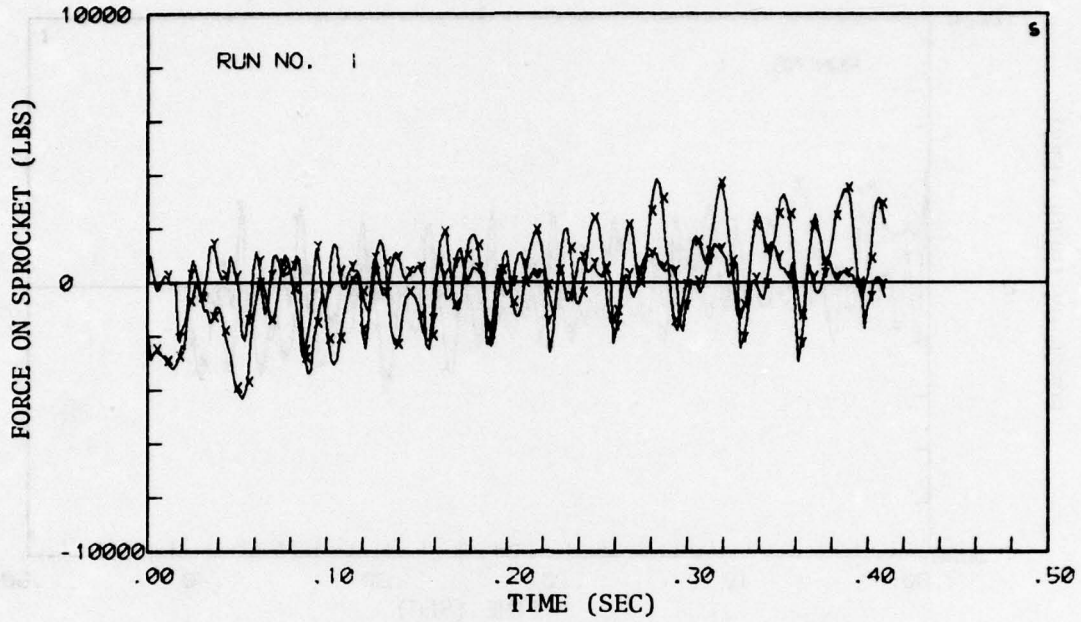

a. Calculated vertical (y) and horizontal (x) force time history on the sprocket

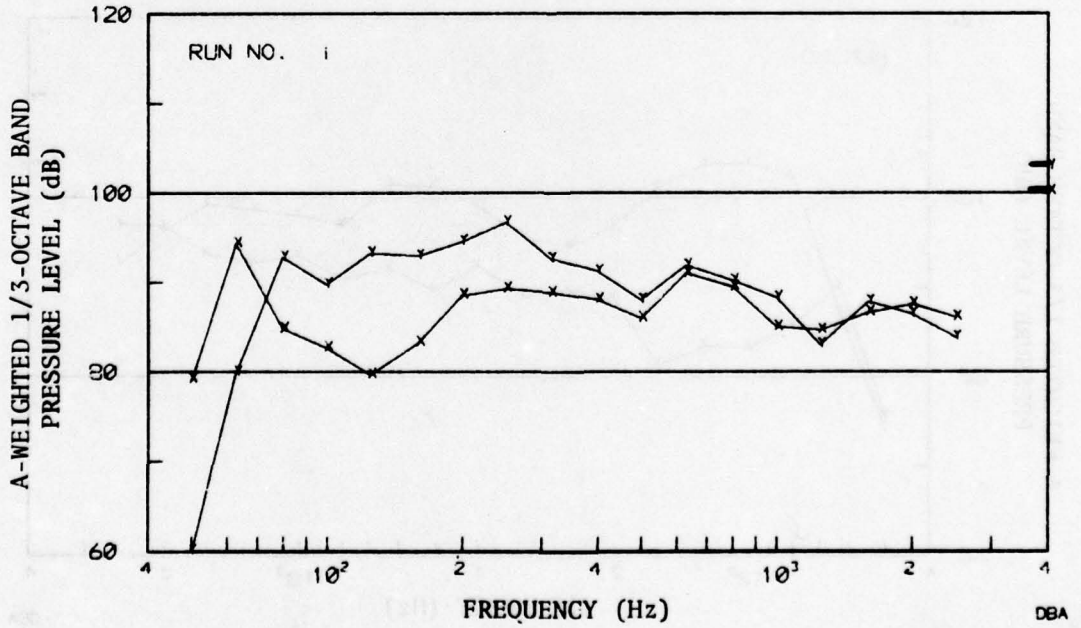

b. Calculated A-weighted 1/3-octave band pressure level and overall A-weighted level (dBA) produced by sprocket

Figure 30. Baseline run, 10 MPH; Calculated sprocket forces and noise spectra.

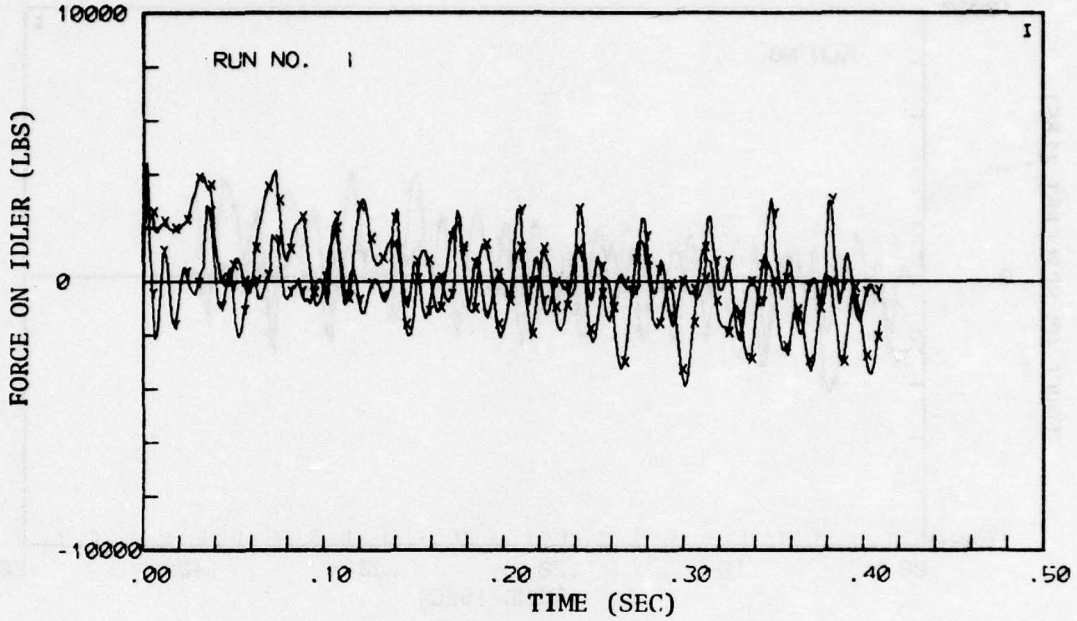

a. Calculated vertical (y) and horizontal (x) force time history on the idler

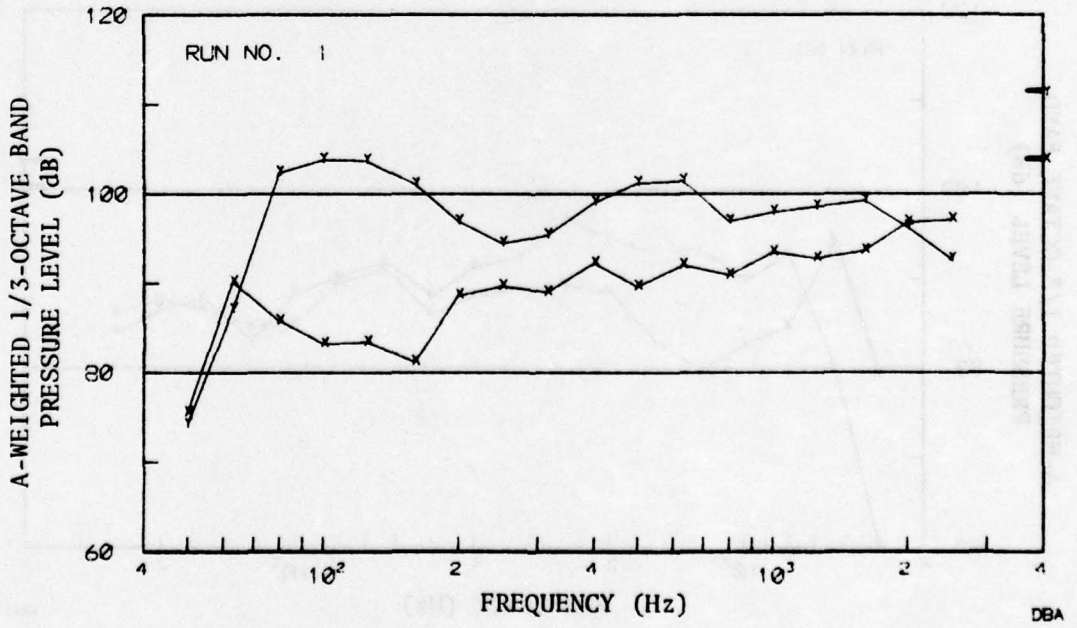

b. Calculated A-weighted 1/3-octave band pressure level and overall A-weighted level (dBA) produced by idler

Figure 31. Baseline run, 10 MPH; Calculated idler forces and noise spectra.

RUN NO. 3

SPROCKET RADIUS	RS	(IN)	=	9.50
IDLER RADIUS	RI	(IN)	=	9.50
TRACK PITCH	L	(IN)	=	6.00
NUMBER OF SHOES	NS		=	65.00
SPROCKET TANGENTIAL STIFFNESS	KST	(KLB/IN)	=	3.00
" " DAMPING COEF.	CST	(LB*SEC/IN)	=	6.52
SPROCKET RADIAL STIFFNESS	KSR	(KLB/IN)	=	3.00
" " DAMPING COEF.	CSR	(LB*SEC/IN)	=	6.52
IDLER TANGENTIAL STIFFNESS	KIT	(KLB/IN)	=	3.00
" " DAMPING COEF.	CIT	(LB*SEC/IN)	=	6.52
IDLER RADIAL STIFFNESS	KIR	(KLB/IN)	=	3.00
" " DAMPING COEF.	CIR	(LB*SEC/IN)	=	6.52
BUSHING STIFFNESS	KB	(KLB/IN)	=	140.00
BUSHING DAMPING COEF.	CBL	(LB*SEC/IN)	=	44.54
BUSHING TORSIONAL STIFFNESS	QQ	(KLB*IN/RD)	=	2.24
SPROCKET COULOMB FRICTION COF.	MUS		=	.30
IDLER COULOMB FRICTION COF.	MUI		=	.30
VEHICLE VELOCITY (MPH)	V	(MPH)	=	10.00
TRACK SHOE MASS	SM	(SLUGS)	=	.63
TRACK SHOE MOMENT OF INERTIA	SMI	(SLG*IN**2)	=	1.87
IDLER MOMENT OF INERTIA	WMI	(SLG*IN**2)	=	146.88
TRACK STRAND TENSION	TNS	(KLBS)	=	3.00
TIME-AV. X-FORCE ON SPROCKET	Q1	(KLBS)	=	7.50
TIME-AV. Y-FORCE ON SPROCKET	Q2	(KLBS)	=	-.03
TIME-AV. X-FORCE ON IDLER	Q3	(KLBS)	=	-7.50
TIME-AV. Y-FORCE ON IDLER	Q4	(KLBS)	=	.01
SAMPLING TIME	TO	(MSEC)	=	.10

Figure 32. Compliant idler and sprocket, 10 MPH; Input data and time averages of X and Y forces on the idler and sprocket wheels.

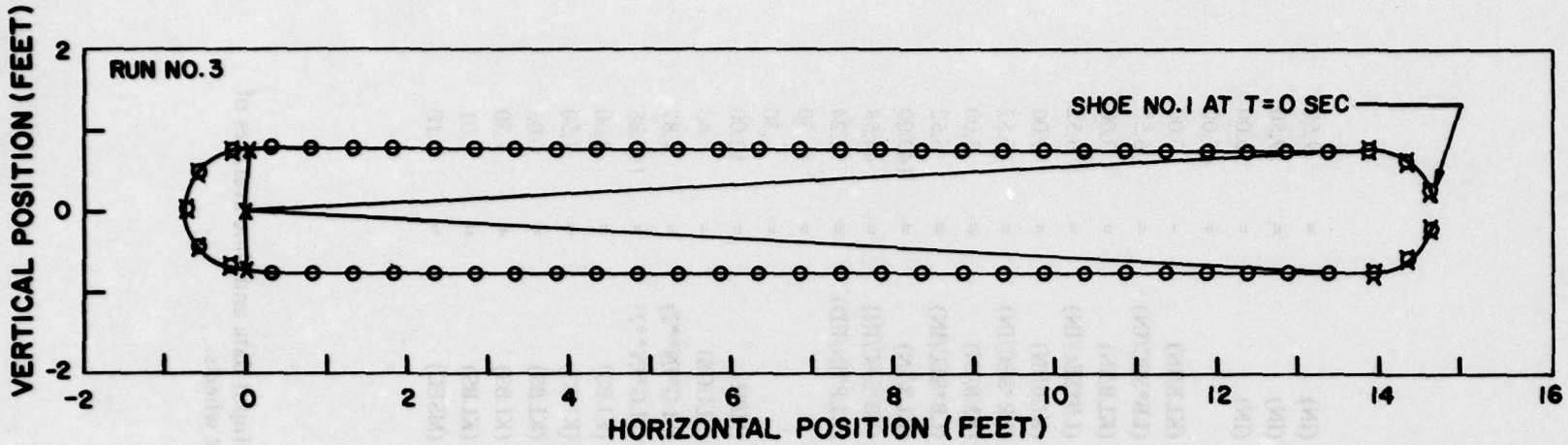

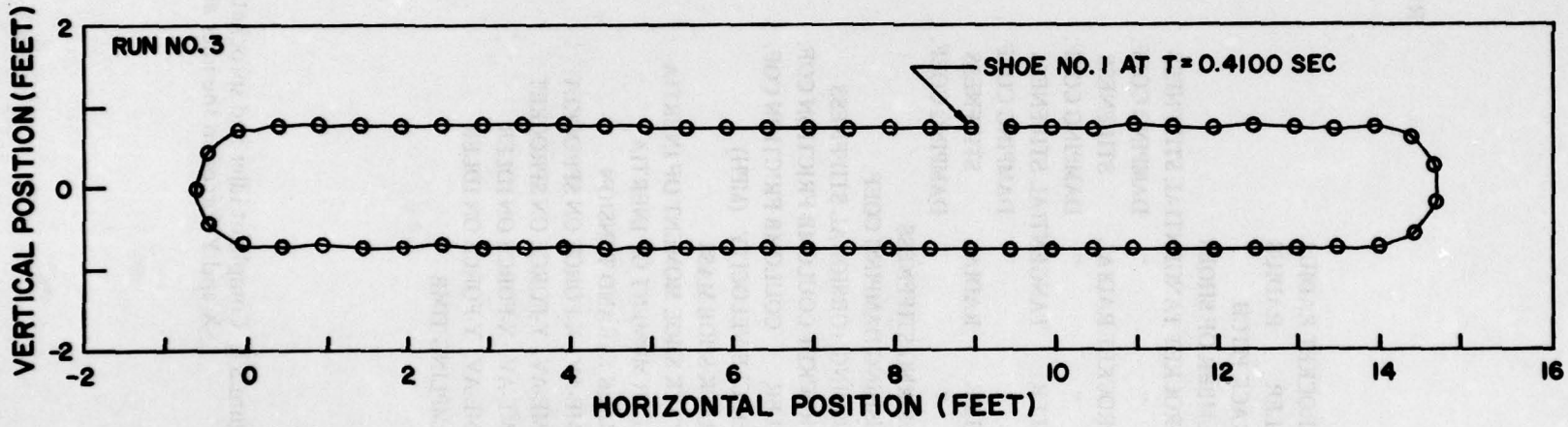

Figure 33. Compliant idler and sprocket, 10 MPH; Diagrams of track shoe positions.

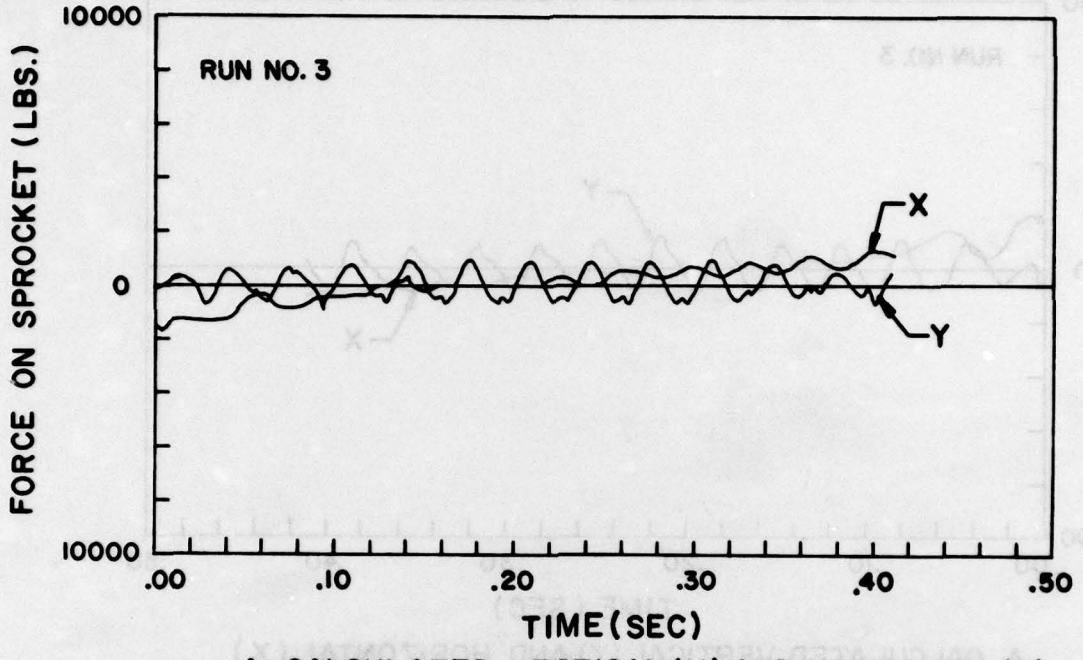

A. CALCULATED VERTICAL (Y) AND HORIZONTAL (X) FORCE TIME HISTORY ON THE SPROCKET

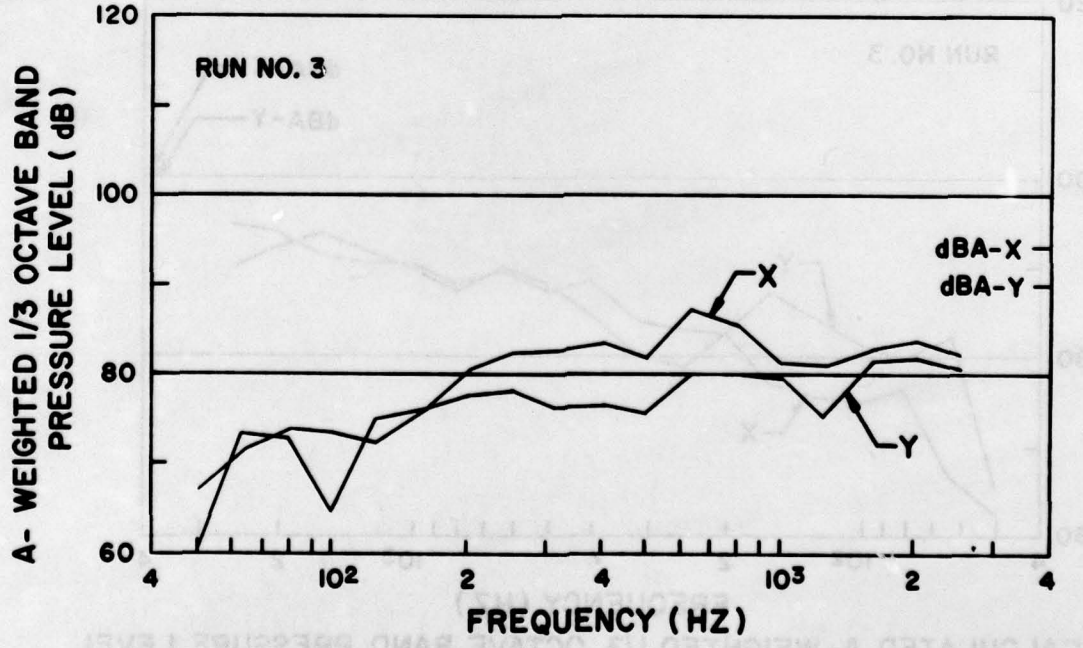

B. CALCULATED A-WEIGHTED 1/3 OCTAVE BAND PRESSURE LEVEL AND OVERALL A-WEIGHTED LEVEL (dBA) PRODUCED BY SPROCKET

Figure 34. Compliant idler and sprocket, 10 MPH; Calculated sprocket forces and noise spectra.

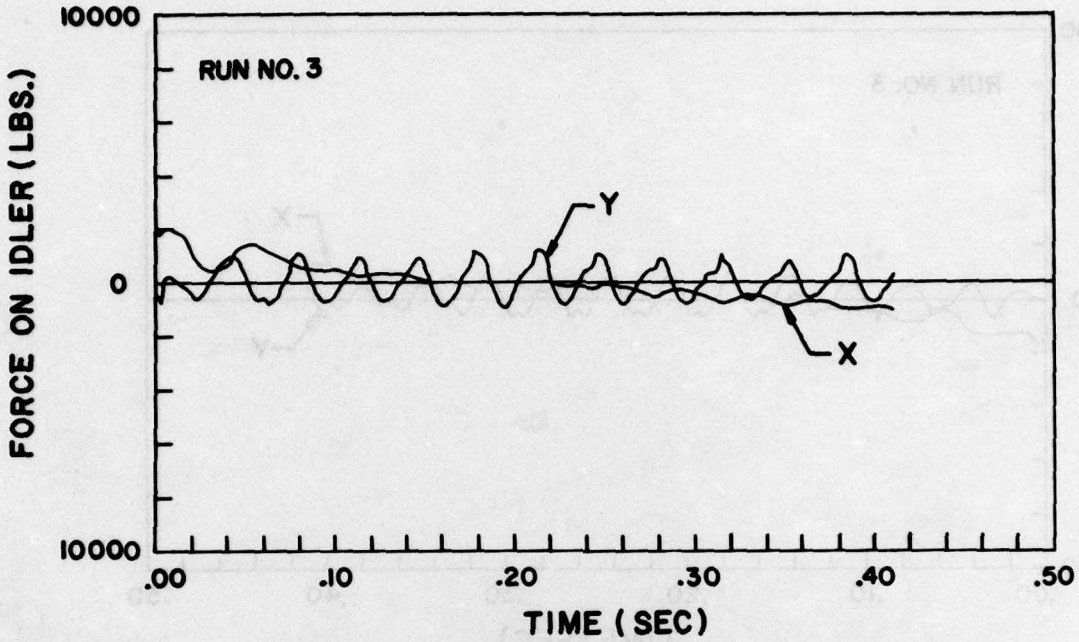

A. CALCULATED VERTICAL (Y) AND HORIZONTAL (X) FORCE TIME HISTORY ON THE IDLER

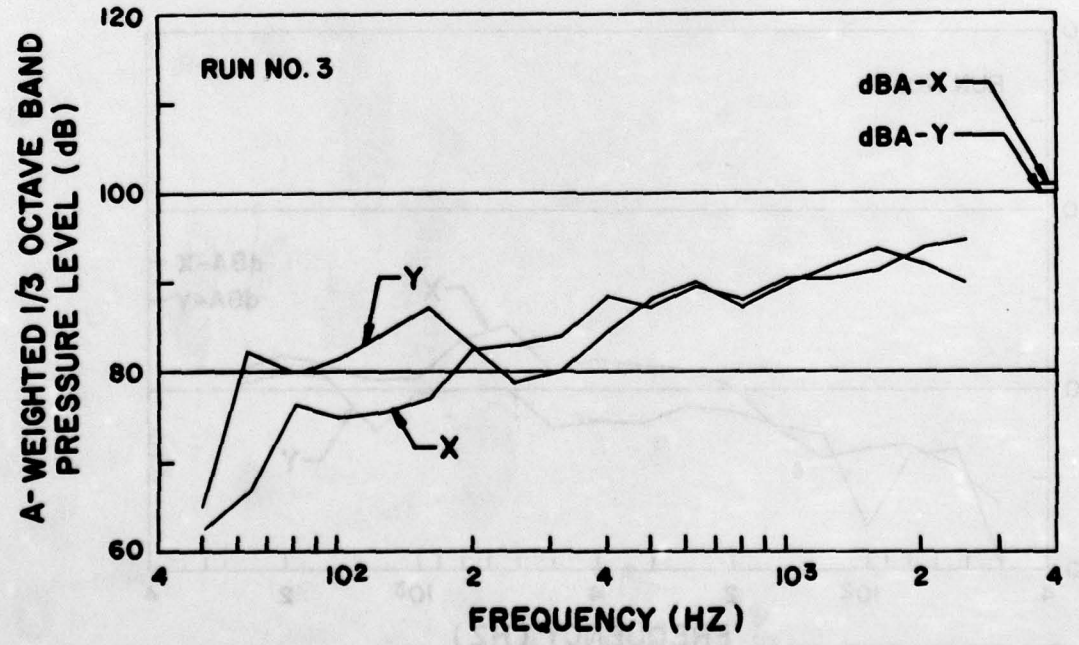

B. CALCULATED A-WEIGHTED 1/3 OCTAVE BAND PRESSURE LEVEL AND OVERALL A-WEIGHTED LEVEL (dBA) PRODUCED BY IDLER

Figure 35. Compliant idler and sprocket, 10 MPH; Calculated idler forces and noise spectra.

RUN NO. 6

SPROCKET RADIUS	RS	(IN)	= 9.50
IDLER RADIUS	RI	(IN)	= 9.50
TRACK PITCH	L	(IN)	= 6.00
NUMBER OF SHOES	NS		= 65.00
SPROCKET TANGENTIAL STIFFNESS	KST	(KLB/IN)	= 12.00
" " DAMPING COEF.	CST	(LB*SEC/IN)	= 13.04
SPROCKET RADIAL STIFFNESS	KSR	(KLB/IN)	= 12.00
" " DAMPING COEF.	CSR	(LB*SEC/IN)	= 13.04
IDLER TANGENTIAL STIFFNESS	KIT	(KLB/IN)	= 12.00
" " DAMPING COEF.	CIT	(LB*SEC/IN)	= 13.04
IDLER RADIAL STIFFNESS	KIR	(KLB/IN)	= 12.00
" " DAMPING COEF.	CIR	(LB*SEC/IN)	= 13.04
BUSHING STIFFNESS	KB	(KLB/IN)	= 140.00
BUSHING DAMPING COEF.	CBL	(LB*SEC/IN)	= 44.54
BUSHING TORSIONAL STIFFNESS	QQ	(KLB*IN/RD)	= 2.24
SPROCKET COULOMB FRICTION COF.	MUS		= .30
IDLER COULOMB FRICTION COF.	MUI		= .30
VEHICLE VELOCITY (MPH)	V	(MPH)	= 30.00
TRACK SHOE MASS	SM	(SLUGS)	= .63
TRACK SHOE MOMENT OF INERTIA	SMI	(SLG*IN**2)	= 1.87
IDLER MOMENT OF INERTIA	WMI	(SLG*IN**2)	= 146.88
TRACK STRAND TENSION	TNS	(KLBS)	= 3.00
TIME-AV. X-FORCE ON SPROCKET	Q1	(KLBS)	= 25.75
TIME-AV. Y-FORCE ON SPROCKET	Q2	(KLBS)	= -.27
TIME-AV. X-FORCE ON IDLER	Q3	(KLBS)	= -25.87
TIME-AV. Y-FORCE ON IDLER	Q4	(KLBS)	= .17
SAMPLING TIME	T0	(MSEC)	= .10

Figure 36. Semi-compliant idler and sprocket, 30 MPH; Input data and time averages of X and Y forces on idler and sprocket.

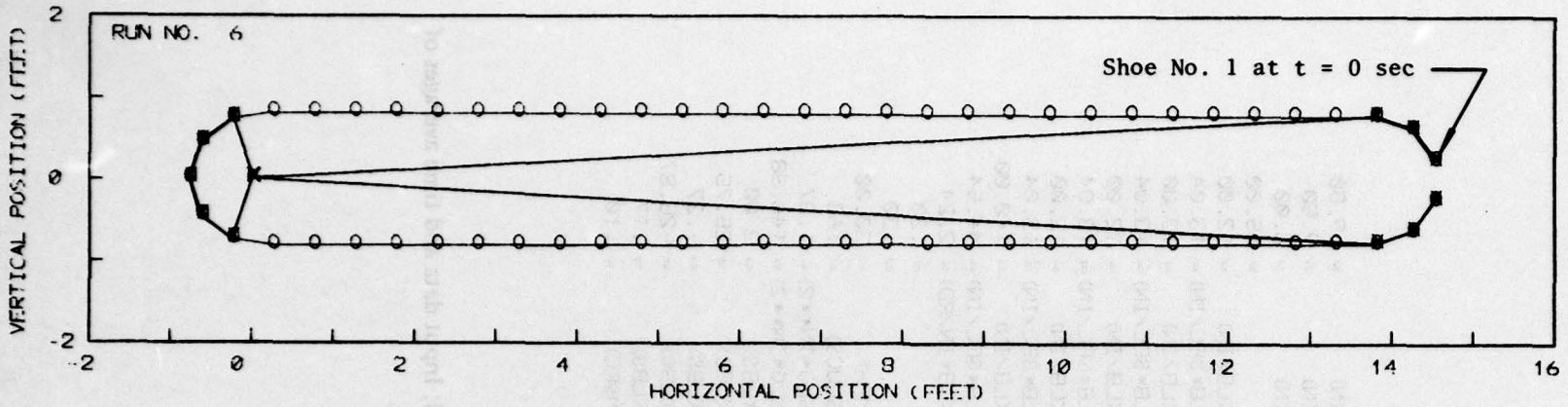

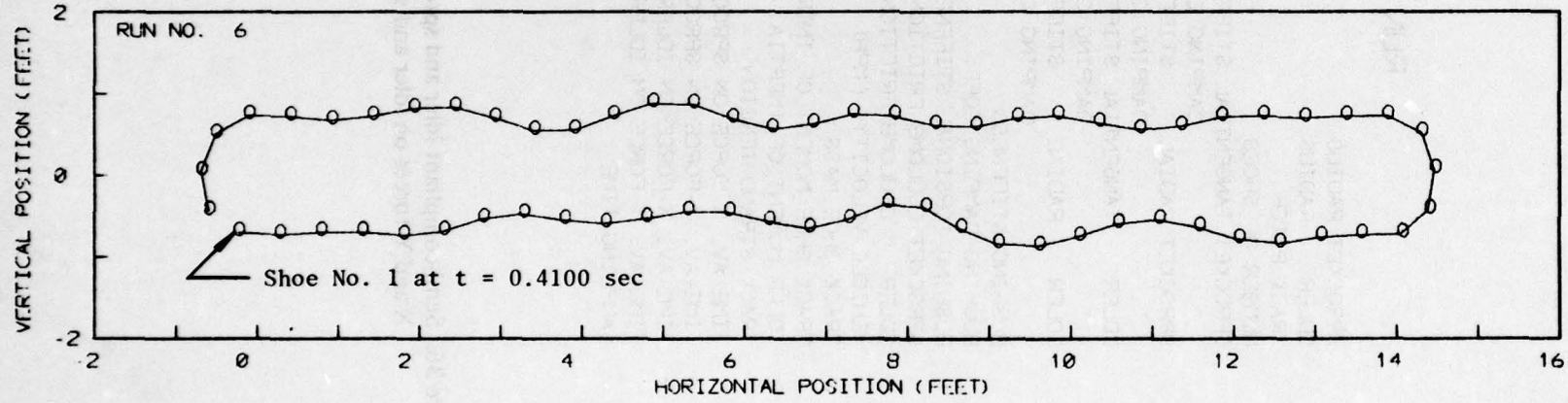

Figure 37. Semi-compliant idler and sprocket, 30 MPH; Diagrams of track shoe positions.

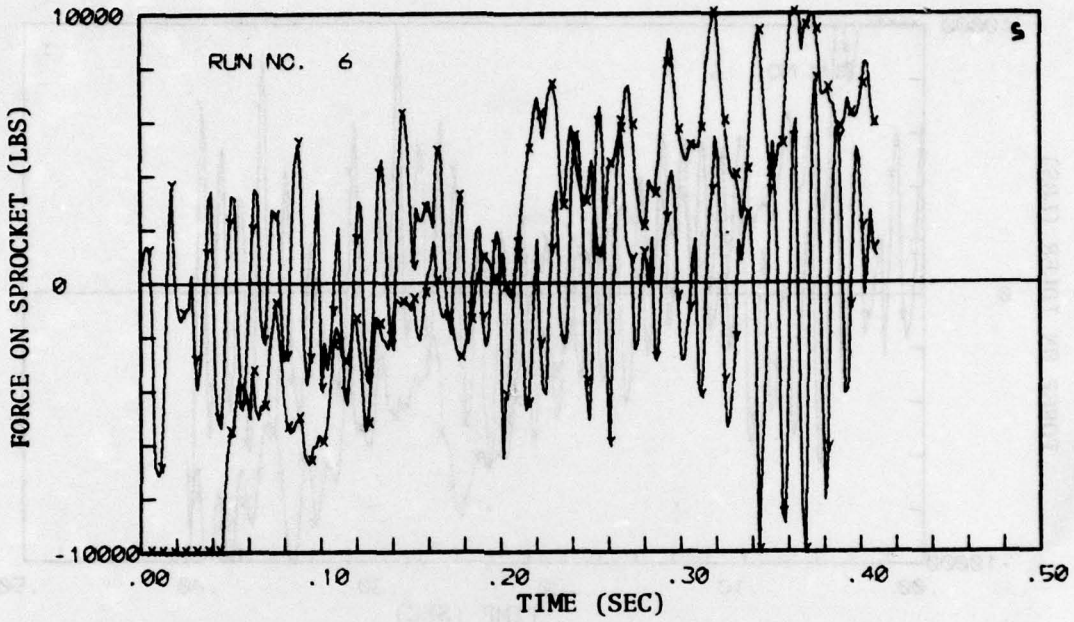

a. Calculated vertical (y) and horizontal (x) force time history on the sprocket

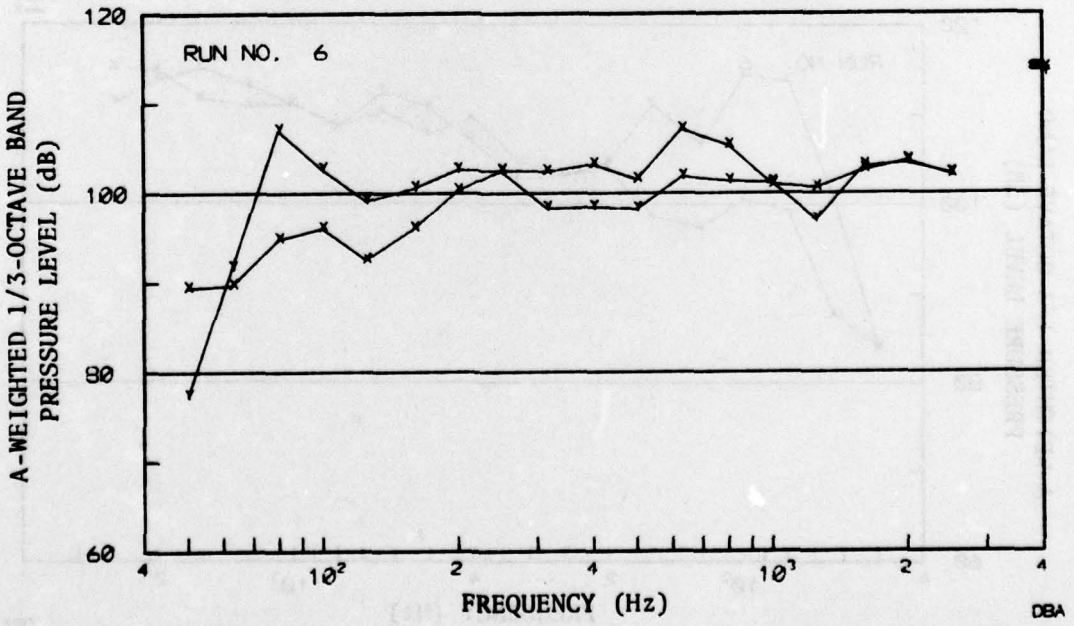

b. Calculated A-weighted 1/3-octave band pressure level and overall A-weighted level (dBA) produced by sprocket

Figure 38. Semi-compliant idler and sprocket, 30 MPH; Calculated sprocket forces and noise spectra.

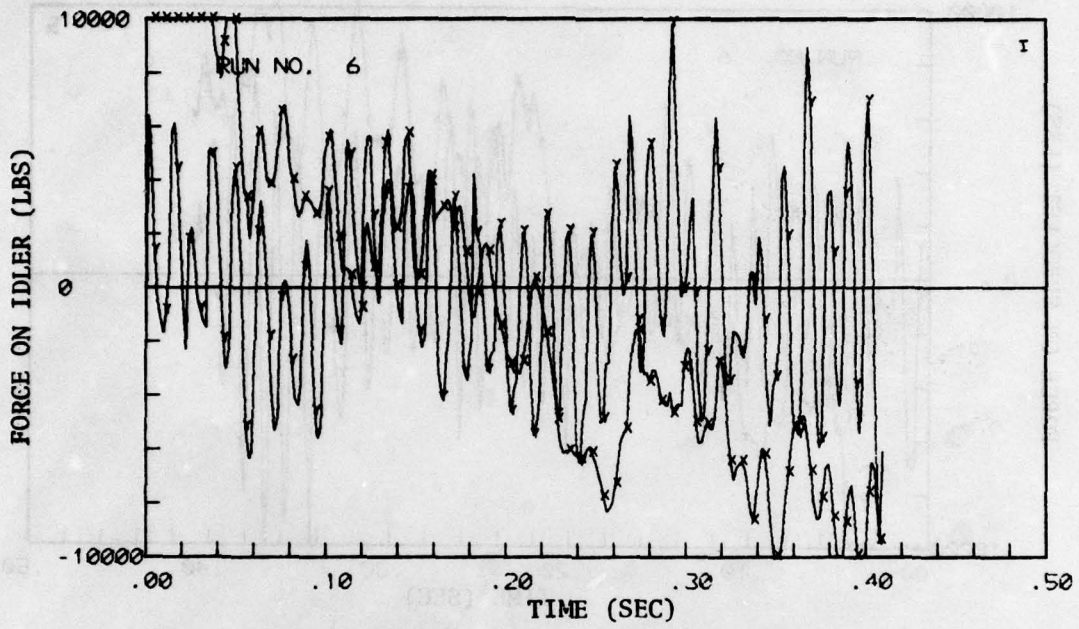

a. Calculated vertical (y) and horizontal (x) force time history on the idler

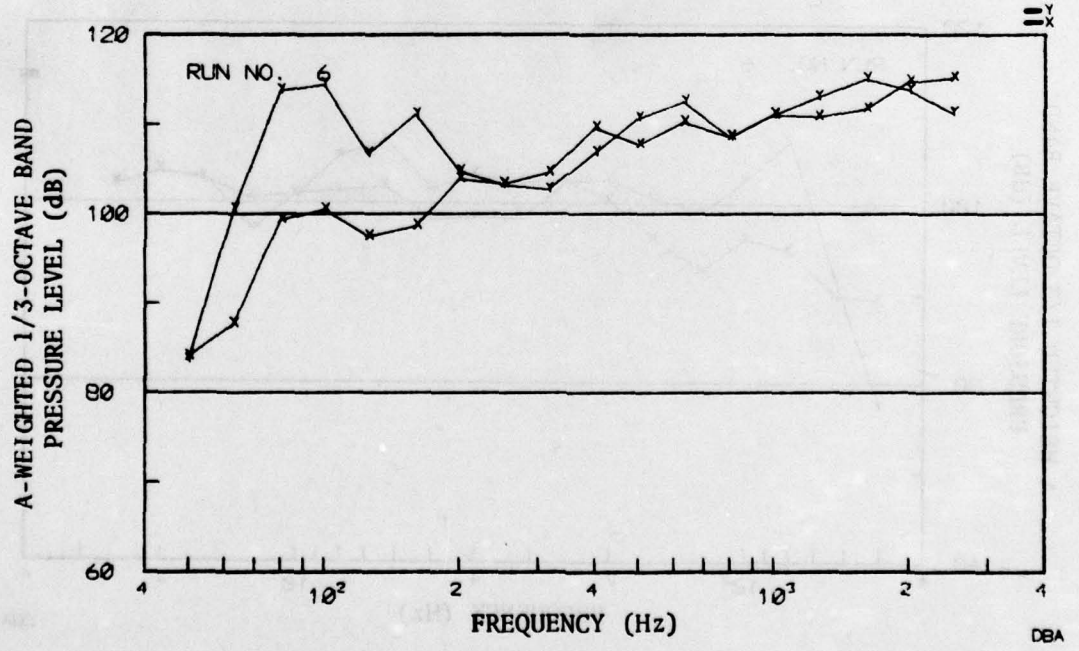

b. Calculated A-weighted 1/3-octave band pressure level and overall A-weighted level (dBA) produced by idler

Figure 39. Semi-compliant idler and sprocket, 30 MPH; Calculated idler forces and noise spectra.

In the third simulation presented, the track speed has been increased from 10 mph to 30 mph, and the wheel stiffnesses set at 12,000 pounds per inch. The importance of the pictorial time histories is very apparent in that near the end of the run in the lower diagram the track undergoes an undulatory motion. Because the centers of the wheels are at fixed distances from each other, the track tension increased from a static tension of 3,000 pounds to a dynamic, time-averaged tension of 12,400 pounds. Since increasing track tension is known to raise interior noise, no conclusions regarding noise can be drawn from this simulation. However, it is apparent that the undulating motion must be eliminated in order to utilize the analysis.

CONCLUSIONS

The conclusions reached in this study are summarized below:

1. The statistical energy analysis of the acoustic and vibratory power flows were self-consistent. That is, the calculated acoustic power radiated into the crew area agrees well with the calculated acoustic dissipation.

2. A damping treatment applied to both sponsons provided appreciable sponson vibration reduction at 500 Hz and higher frequencies. This treatment also gave a modest vibration reduction of other hull plates, and noise reduction of approximately 0-2 dB(A).

3. Very careful control of testing parameters is necessary to accurately measure the incremental noise reductions that must be evaluated, such as would be necessary to confirm the above estimated noise reduction.

4. To achieve appreciable noise reduction by means of hull plate damping, a promising technique is constrained layer damping.

5. A damping treatment of the roadwheels was found to reduce roadwheel resonant amplitudes when vibrated by an electrodynamic shaker. Further experimentation is needed to determine if a corresponding crew area noise reduction could be obtained.

6. Local stiffening of the hull at the roadarm and idler mounting locations provided no significant changes to the mechanical impedances and, therefore, no noise reduction potential.

7. Vehicle interior sound absorptive treatments are not practical.

8. A very compliant low-noise idler wheel was designed, fabricated, and found to be rugged enough for extensive acoustical testing. Preliminary measurements suggest that the compliant wheel is about 10 dB(A) quieter than the standard idler wheel.

9. The best spring material for compliant idlers and sprockets appears to be either natural or synthetic base "natural" rubber. Steel springs would be difficult to engineer into the limited space available.

10. A number of highly resilient elastomers were also evaluated as spring materials, but were found to have inferior mechanical or damping properties.

11. In the compliant idler wheel, side-to-side as well as radial and tangential compliance must be considered.

12. The computerized simulation of track dynamics, while producing promising results, would require incremental refinement before it should be used in designing lower noise suspension components.

Based on these conclusions, a quieted demonstration vehicle might include compliant idler and sprocket wheels to reduce hull force inputs, a hull damping treatment to reduce hull vibration and a modified hull structure to reduce both hull vibration and noise radiated into the occupied areas.

REFERENCES

1. Bates, C.L., & Sparks, C.R. Development of measurement techniques for the analysis of tracked vehicle vibration and noise. SWRI Project No. 04-1421, Contract DA 23-072-AMC-144(T), Southwest Research Institute, October 1964.

2. Benson, G.L. T91E3 type rubber mounted sprockets with Harris Products Co. No. 69001 rubber bushings. Report No. 137, Test and Development Department TE-20, Cadillac Motor Car Division, General Motors Corporation, Cleveland Tank Plant, June 17, 1952.

3. Beranek, L.L. (Ed.) Noise and vibration control. Chapter 11. New York: McGraw-Hill Book Co., 1971.

4. Bibbens, R.N. Return idler wheels: Various designs compared for durability and effect on vehicle noise and vibration levels. FMC OED Technical Report 722, Ordnance Engineering Division, FMC Corporation, October 1969.

5. Department of Defense. Military standard noise limits for Army materiel. MIL-STD-1474B(MI), Washington, DC 20301. (Obtain from the Naval Publications and Forms Center, 5801 Tabor Avenue, Philadelphia, PA 19120.)

6. Galaitsis, A.G. Phase II: Track vehicle dynamics analysis. BBN Report 3919, Contract DAA05-77-C-0729, September 1978.

7. Hammond, S. AIFV informal data transmission on interior noise levels. Ordnance Engineering Division, San Jose, CA, to Peter Rentz of Bolt Beranek and Newman, Inc. of Canoga Park, CA, October 17, 1978.

8. Hammond, S. M113A1 idler heat rejection. Technical Report 3171, FMC Corporation, San Jose, CA, July 1977.

9. Hare, R.B. MICV XM 723 test report: Internal noise survey of the prototype vehicle. FMC OED Technical Report 2762 Contract DAA-E07-73-C-0100, Ordnance Engineering Division, FMC Corporation, October 1974.

10. Hoberecht, I.W. Durability test of International Harvester rubber tired hub and sprocket assemblies. Report No. 850, Test and Development Department TE-20, Cadillac Motor Car Division, General Motors Corporation, Cleveland Tank Plant (Test requested by International Harvester Company for M75 vehicle), May 20, 1954.

11. Holland, H.H., Jr. Noise levels in the passenger areas of a standard and a product improved M113A1 armored personnel carrier. Letter Report No. 124, U.S. Army Human Engineering Laboratory, Aberdeen Proving Ground, MD, October 1970.

12. Hurst, F.L. Comparison (IC) test of carrier, personnel, full-track, armored M113A1. YGP Report No. 8031, USATAC Project No. QKP-IC-T-68-Y17, December 1968. (AD No. 846351L)

13. Lenert, R.P. Engineering Testing Division Automotive Branch report on noise and vibration test of M113 armored personnel carrier with standard and short pitch tracks. Report No. DPS/OTA-166, Ordnance Test Activity, Development and Proof Services, Aberdeen Proving Ground, MD, September 1962.

14. Lyon, R.H. Statistical energy analysis of dynamical systems: Theory and applications. Cambridge, MA & London: MIT Press, 1975.

15. Maidanik, G. Response of ribbed panels to reverberant acoustic fields. Journal of Acoustical Society of America, 1962, 34, 809-826.

16. Norris, T.R., Hare, R.B., Galaitsis, A.G., & Garinther, G.R. Development of advanced concepts for noise reductions in tracked vehicles. Technical Memorandum 25-77, US Army Human Engineering Laboratory, Aberdeen Proving Ground, MD, August 1977.

17. Norris, T.R. Tracked vehicles: Noise and vibration control study using a reduced scale model. BBN Technical Report No. 3031, Bolt Beranek and Newman, Inc., San Francisco, CA. Prepared for Mr. Donald Rees, US Army Tank Automotive Command, Warren, MI 48090, Report 12099.

18. Prior, J.R. Vibration comparison of four types of tracks. Test and Development Department TE-20, Cadillac Motor Car Division, General Motors Corporation, Cleveland Tank Plant, January 12, 1956. (Report 1203.)

19. Rees, D.W. Changes in vehicle noise level brought about by installation of modified track roadwheels. TACOM Report 11971, 1974.

20. Rentz, P.E. Hull vibratory power flow and resulting interior noise on the M113A1 armored personnel carrier. Presented at the 48th Symposium on Shock and Vibration, Huntsville, AL, October 18-20, 1977.

21. Sobszyk, J.P. Automotive Division report on component development test of wire-link track, tested in comparison with Standard T130 forged track. Report No. DPS-850, DA Project No. 548-12-001, Development and Proof Services, Aberdeen Proving Ground, MD, February 1963.

22. The Goodyear Tire & Rubber Company. Handbook of molded and extruded rubber. (3d ed.). Akron, Ohio 44316.

23. Van Wyk, T. B. Study of track-idler engagement and its effect on interior noise. Technical Report 2976, FMC Corporation, San Jose, CA, April 1976.

24. Wiley, J.R. XM551 noise reduction program-Phase I. MPG187, P.O. No. NEP-63571-KM and NEP-63570-KM, General Motors Proving Ground, Milford, MI, June 13, 1966.

25. Young, W.J. Rubber tired sprocket hub (International Harvester Company design) effect on T141 vehicle vibration. Report 1201, Test and Development Department TE-20, Cadillac Motor Car Division, General Motors Corporation, Cleveland Tank Plant, March 11, 1954.

APPENDIX

PRINCIPLES OF STATISTICAL ENERGY ANALYSIS SUMMARIZED

Principles of Statistical Energy Analysis Summarized

In vibro-acoustic systems with several modes in the frequency bands of interest, it is convenient, and often more accurate, to deal with time and frequency band averaged characteristics. This practical approach has been developed and extensively applied to room acoustics problems. More recently, the approach has been applied to vibrating structures and to the interaction of the vibrating structures and surrounding fluid fields. This discipline has been named Statistical Energy Analysis (SEA) and is summarized in various references (3, 14).

The vibratory and acoustic power flow relations which have been utilized in this study fall into four categories: structural dissipation, panel radiation, reverberant room acoustics, and power flow into a structure.

Structural Dissipated Power

The vibratory power dissipated in a structure is given by:

$$W_d = 2\pi f \eta \langle v^2 \rangle m \qquad (1)$$

Where W_d = power dissipated ft-lb/sec

f = frequency, Hz

η = internal loss factor

v = velocity, ft/sec

m = structure mass lb sec^2/ft

In engineering form:

$$PWL = AL + 10 \log \frac{\eta w}{f} + 128.4 \qquad (2)$$

Where $AL = 10 \log \frac{\langle a^2 \rangle}{g^2}$ = acceleration level, dB re 1.0g

a = acceleration, ft/sec^2

w = weight, lbs

PWL = power level, dB re 10^{-12} watt

$g = 32.2$ ft/sec^2

Radiated Sound Power

The power radiated from a plate can also be estimated from measured plate acceleration levels. The time averaged total power, W_r, radiated from a plate is in ft-lb/sec:

$$W_r = R_{rad} \langle a^2 \rangle / 4\pi^2 f^2 \qquad (3)$$

In this equation, R_{rad} is the radiation resistance of the plate and $\langle a^2 \rangle$ is the space averaged mean square acceleration level in the band centered at frequency f. The radiation resistance is:

$$R_{rad} = \rho c S \sigma \qquad (4)$$

Here, ρc is the characteristic acoustic impedance of the air, S is the total radiating area, and σ is the radiation efficiency.

The radiation efficiency is a function of the critical frequency of the plates and of a nondimensional parameter $\beta = Ph/S$. P is twice the total length of all stiffeners on the surface of area S plus the boundary length enclosing S and h is the thickness of the plate thus enclosed. The critical frequency is the frequency at which the bending wavelength in the plate equals the acoustic wavelength in the air and is (for aluminum plates):

$$f_c = 41.3/h$$

where h = thickness, feet.

Again, the acceleration level, AL, of a plate is related to the mean square acceleration by:

$$AL = 10 \log \langle a_s^2 \rangle / g^2 \qquad (5)$$

By substituting Equations (4) and (5) into (3), the radiated sound power level in dB re 10^{-12} watts by plates of total area S can be expressed as:

$$PWL_{rad} = AL + 10 \log \sigma S - 20 \log f + 139.7 \qquad (6)$$

Resulting Sound Power in an Acoustic Space

For a reverberant space, with air as the fluid:

$$PWL = SPL + 10 \log \left(\frac{R}{4}\right) - 10 \qquad (7)$$

where SPL = space averaged sound pressure level,

$R \simeq \frac{0.049V}{T_{60}}$ = room constant, ft^2

V - volume, ft^3

T_{60} = Reverberation time, seconds

or, directly in terms of the reverberation time:

$$PWL = SPL + 10 \log \frac{V}{T_{60}} - 29 \qquad (8)$$

Vibratory Power Injected Into a Structure

The input vibratory power depends on the characterization of the source. Given the velocity at the point of attachment:

$$W_{in} = Re \left[Z \langle v^2 \rangle \right] = |Z| \langle v \rangle^2 \cos \xi \qquad (9)$$

where Z = Point mechanical impedance, $\frac{lb\ sec}{ft}$

v = Point velocity, ft/sec

ξ = Phase angle between force and velocity, degrees

In engineering terms, and using the interance phase angle

$$PWL_{in} = 10 \log |Z| + AL - 20 \log f + 10 \log \cos \xi + 135.5 \qquad (10)$$

where ξ is the phase angle between force and acceleration, in degrees.

Alternately, given the force at the point of attachment

$$W_{in} = Re \frac{\langle F^2 \rangle}{Z} = \frac{\langle F^2 \rangle \cos \xi}{|Z|} \qquad (11)$$

where F = force, lbs

In engineering terms

$$PWL = 10 \log \langle F^2 \rangle - 10 \log |Z| + 10 \log \cos \xi + 121.3 \qquad (12)$$

Application to M113A1 Hull and Suspension

Most of the quantities required are directly measurable. One exception is the radiation efficiency of the hull panels which are well coupled to each other. For the major panels, the radiation efficiency was determined analytically from work of Maidanik (15). In addition, individual panel loss factor values are generally not measurable. Therefore, the total vehicle loss factor was measured and used for calculations involving each individual panel. With the coupling values between the panels estimated to be greater than the individual panel loss factor values, this approximation is considered valid.

SUPPLEMENTARY

INFORMATION

DEPARTMENT OF THE ARMY
U.S. ARMY HUMAN ENGINEERING LABORATORY
ABERDEEN PROVING GROUND, MARYLAND 21005

ERRATA SHEET
for

US Army Human Engineering Laboratory Technical Memorandum 8-79, entitled "Experimental Idler Design and Development of Hull Concepts for Noise Reduction in Tracked Vehicles," June 1979.

Add Page 4.

PREFACE

During the course of the noise reduction program, the US Army Human Engineering Laboratory has received invaluable technical assistance from Jiro Adachi of AMMRC, Felix Sachs of AEHA and Don Rees of TARADCOM. We are deeply indebted to these individuals for the advice provided in their respective areas of expertise and for their attendance and contributions at meetings. We are particularly thankful to TARADCOM for their encouragement through the past two phases and for their plans to support the program with funding during succeeding phases.